Pergamon

Int. J. Solids Structures Vol. 35, Nos 9–10, pp. 855–887, 1998

0020–7683/98 $19.00 + .00

PII: S0020–1008(97)00088–7

FINITE ELEMENT SIMULATION OF MARTENSITIC PHASE TRANSITIONS IN ELASTOPLASTIC MATERIALS

V. I. LEVITAS, A. V. IDESMAN and E. STEIN
University of Hannover, Institute of Structural and Computational Mechanics, Appelstr. 9A, 30167 Hannover, Germany

(*Received* 12 *August* 1996; *in revised form* 19 *March* 1997)

Abstract—A problem formulation for a continuum thermomechanical description of martensitic phase transitions (PT) in elastoplastic materials is presented. Stress history dependence, during the transformation process, is a characteristic feature of the new PT criterion. Relatively simple mechanical models for noncoherence and fracture at interfaces are proposed. Solution algorithms (which include, in particular, the solution of standard elastoplastic contact problem) and numerical results for elastoplastic model problems with PT (noncoherent interface, interface with fracture, moving interface, progress of PT zone) are presented. It is shown that: (a) a noncoherent interface and fracture promote considerably nucleation; (b) a noncoherent interface has low mobility or cannot move at all which agrees with known experiments; (c) for elastic materials the growth of a single connected region of new phase occurs; for elastoplastic materials complex multiple connected PT region (discrete microstructure) is obtained. © 1997 Published by Elsevier Science Ltd.

1. INTRODUCTION

Phase transitions (PT) in elastoplastic materials play a significant role in a lot of advanced technical problems, e.g. for thermomechanical treatment of metals, for transformation-induced plasticity phenomenon and others. Martensitic PT in elastoplastic materials is a complex thermomechanical process accompanied by the change of mechanical properties, transformation strain and a complicated distribution of local stresses and strains. The difficulties of a thermomechanical description of PT are related to the definition of the PT condition, formulation of boundary value problem and its numerical solution.

Various types of numerical methods for PT in elastoplastic materials are known. The peculiarity of stress–strain state during the PT without thermodynamical description was treated by Leblond *et al.* (1989) and Mitter (1987). Simulation of PT-kinetics in terms of volume fraction of new phase is considered by Inoue and Raniecki (1978), Novikov *et al.* (1988, 1991), Levitas *et al.* (1989), Stringfellow *et al.* (1992), Simonsson (1994) and Denis (1996). Such descriptions are not the topic of our paper.

We will consider the instantaneous occurrence of PT in some volume based on thermodynamics, without the introduction of volume fraction and prescribing the kinetic equations. There are only two known numerical approaches of such type for PT in elastoplastic materials. Ganghoffer *et al.* (1991) and Marketz and Fischer (1994a, 1994b) used FEM to model PT progress in a grain (appearance of martensitic plates). Typical of these papers is that the PT conditions for elastoplastic materials are not related directly to the second law of thermodynamics and the dissipation due to the PT. That is why it is difficult to understand the physical sense of these conditions and to choose which one is correct and which not.

In papers by Levitas (1995a, 1995b, 1995c, 1996, 1997a, 1997b) a new thermomechanical description of PT in elastoplastic materials, based on the second law of thermodynamics, was proposed. The goal of this paper is to show how this new PT criterion can be used for computations using the finite element method and which features of PT can be described by it. We will not consider here crystallographic peculiarities of PT, but deal with dilatational transformation strain only. New condition of nucleation (which also differs from known approaches) includes the history of local stresses variation in nucleus

during the transformation process. Therefore, knowledge of stresses and strains before and after PT does not give sufficient information to calculate PT conditions. This fact causes additional difficulties for the numerical method. At first, we will consider the formulation of an elastoplastic problem with PT based on the new PT criterion and related maximum principle. Then we will consider the simplest model problem with a given PT region and will calculate the condition for PT in this region (i.e. inverse problem is solved) and will investigate the progress of plastic strains (TRIP) in elastoplastic sample under cyclic appearance and disappearance of new phase nucleus at fixed external force. Within this formulation we show a simple way of admitting noncoherence (sliding) and fracture at the fixed and moving interfaces between new and old phases. It will be shown that noncoherence and fracture at the interface considerably change the PT process. Then the simulation of PT progress, based on the maximum principle for PT, will be considered. Element by element technique is used to model PT progress. It will be shown that for elastic materials the growth of a single connected region of a new phase occurs; for elastoplastic materials complex multiple connected PT region (discrete microstructure) is obtained. All the model problems under consideration are axisymmetric and restricted to small strains. To calculate the PT conditions for the above problems, elastoplastic contact problems are solved by FEM [Idesman and Levitas (1995)] to determine variation of local stresses as a function of growing transformation strain.

2. THERMOMECHANICAL THEORY OF PT

2.1. *Phase transition criterion*

Let us consider a volume, V, of a multiphase material with prescribed boundary data on a surface S. Assume that in some volume $V_n \in V$ with the boundary Σ_n a PT occurs in time Δt. We use the second law of thermodynamics for each point of a volume V_n in the form of the Plank inequality

$$\mathscr{D} = \boldsymbol{\sigma} : \dot{\boldsymbol{\varepsilon}} - \rho\dot{\psi} - \rho s\dot{\theta} \geqslant 0. \tag{1}$$

Here, $\mathscr{D}$ is the rate of dissipation per unit volume, ρ is the mass density, s is the entropy, ψ is the specific Helmholtz free energy, $\boldsymbol{\sigma}$ and $\boldsymbol{\varepsilon}$ are the stress and strain tensors and θ is the temperature. PT is considered as a thermomechanical process of growth of transformation (Bain) strain from the initial to the final value, which is accompanied by a change in all the material's properties. Small strains and linear decomposition of total strain $\boldsymbol{\varepsilon}$ are assumed:

$$\boldsymbol{\varepsilon} = 1/2(\nabla\mathbf{u} + \nabla\mathbf{u}^{\mathrm{T}}) = \boldsymbol{\varepsilon}_{\mathrm{e}} + \boldsymbol{\varepsilon}_{\mathrm{p}} + \boldsymbol{\varepsilon}_{\mathrm{t}}, \tag{2}$$

where $\boldsymbol{\varepsilon}_{\mathrm{e}}$, $\boldsymbol{\varepsilon}_{\mathrm{p}}$ and $\boldsymbol{\varepsilon}_{\mathrm{t}}$ are elastic, plastic and transformation strains, respectively, $\mathbf{u}$ is the displacement vector and ∇ is the gradient operator. The total dissipation increment during the PT in each transforming material point is defined as follows:

$$N := \int_t^{t+\Delta t} \mathscr{D}\,\mathrm{d}t = \int_{\varepsilon_1}^{\varepsilon_2} \boldsymbol{\sigma} : \mathrm{d}\boldsymbol{\varepsilon} - \Delta\psi - \int_{\theta_1}^{\theta_2} \rho s\,\mathrm{d}\theta, \tag{3}$$

where $\Delta\psi = \rho(\psi_2 - \psi_1)$, indices 1 and 2 correspond to the beginning and the end of PT. Assume that during PT two dissipative processes occur: PT itself and plastic flow. The dissipation increment in the course of PT due to plastic flow (when the free energy is independent of $\boldsymbol{\varepsilon}_{\mathrm{p}}$) can be given as

$$N_{\mathrm{p}} = \int_{\varepsilon_{\mathrm{p}1}}^{\varepsilon_{\mathrm{p}2}} \boldsymbol{\sigma} : \mathrm{d}\boldsymbol{\varepsilon}_{\mathrm{p}}. \tag{4}$$

The dissipation increment X due to a PT itself (the driving force for the PT) is a difference

between N and N_p. Neglecting the temperature variation during the PT (the isothermal process is assumed) we have

$$X := N - N_p = \int_{\varepsilon_1}^{\varepsilon_2} \boldsymbol{\sigma} : d(\boldsymbol{\varepsilon}_e + \boldsymbol{\varepsilon}_t) - \Delta\psi. \tag{5}$$

The simplest assumption that both dissipative processes are mutually independent results in conditions that the dissipation increment due to each of dissipative processes should be non-negative, in particular $X \geqslant 0$. Consequently, at $X < 0$ PT is impossible. The condition $X = 0$ is the criterion of PT without dissipation due to PT, because PT is possible (non-contradicts the second law of thermodynamics) and the dissipation increment due to PT is zero. Since practically all martensitic transformations, even in elastic materials, are accompanied with a dissipation and a hysteresis, the PT criterion has the form

$$X = k. \tag{6}$$

Here, k is an experimentally determined value of dissipation due to PT, which can depend on parameters θ, ε_p, ... At $X < k$ PT is impossible.

Let PT occur in some volume V_n (nuclei) and for each point of nuclei V_n PT criterion (6) should be met. Integrating this criterion over the volume V_n we obtain the *nucleation* condition

$$\int_{V_n} X \, dV_n = \int_{V_n} k \, dV_n, \tag{7}$$

or taking into account eqn (5) for X we have

$$\int_{\varepsilon_1}^{\varepsilon_2} \int_{V_n} \boldsymbol{\sigma} : d(\boldsymbol{\varepsilon}_e + \boldsymbol{\varepsilon}_t) \, dV_n - \int_{V_n} \Delta\psi \, dV_n - \int_{V_n} k \, dV_n = 0. \tag{8}$$

Equation (8) has the same form for PT in elastic and elastoplastic materials; plasticity affects a variation of $\boldsymbol{\sigma}$ in the course of PT and the value k. If

$$\rho\psi_i = 0.5\boldsymbol{\varepsilon}_{ei} : \mathbf{E}_i : \boldsymbol{\varepsilon}_{ei} + \rho\psi_i^\theta, \quad i = 1, 2 \quad \text{and} \quad \mathbf{E}_1 = \mathbf{E}_2, \tag{9}$$

where $\mathbf{E}_i$ are the tensors of elastic modules of i-phase, ψ_i^θ is the thermal part of the free energy, then

$$\int_{\varepsilon_{e1}}^{\varepsilon_{e2}} \boldsymbol{\sigma} : d\boldsymbol{\varepsilon}_e = \int_{\varepsilon_{e1}}^{\varepsilon_{e2}} \boldsymbol{\varepsilon}_e : \mathbf{E} : d\boldsymbol{\varepsilon}_e = 0.5(\boldsymbol{\varepsilon}_{e2} : \mathbf{E} : \boldsymbol{\varepsilon}_{e2} - \boldsymbol{\varepsilon}_{e1} : \mathbf{E} : \boldsymbol{\varepsilon}_{e1}) \tag{10}$$

and

$$\int_{V_n} \int_{\varepsilon_{t1}}^{\varepsilon_{t2}} \boldsymbol{\sigma} : d\boldsymbol{\varepsilon}_t \, dV_n - \int_{V_n} \Delta\psi^\theta \, dV_n - \int_{V_n} k \, dV_n = 0,$$

i.e. the elastic strains also disappear. For case of pure dilatational transformation strain it holds $\boldsymbol{\varepsilon}_t = \varepsilon_0 \mathbf{I}$, where $\mathbf{I}$ is a unit tensor, $3\varepsilon_0$ is a volumetric transformation strain. In this case we get $\boldsymbol{\sigma} : d\boldsymbol{\varepsilon}_t = 3\sigma_0 \, d\varepsilon_0$, where σ_0 is the hydrostatic pressure. If the volumetric transformation strain, temperature and k (we assumed that k is function of temperature only) are distributed homogeneously in the nucleus, eqn (10) can be transformed into the following form:

$$\bar{X} := \int_0^{\varepsilon_{02}} 3\bar{\sigma}_0 \, \mathrm{d}\varepsilon_0 - \Delta\underline{\psi}^\theta = k, \quad \bar{\sigma}_0 = \frac{1}{V_n}\int_{V_n} \sigma_0 \, \mathrm{d}V_n, \tag{11}$$

where $\bar{\sigma}_0$ is the averaged over the nucleus pressure and $\bar{X}$ is the driving force of PT (averaged over the nucleus value of X). Equation $(11)_1$ is a final form of phase transformation criterion which is used in the present paper. The integral in eqn $(11)_1$ is calculated numerically after the solution of a set of boundary-value problems using finite element method. The explicit expression for ψ_i^θ can be adopted in the following form [Huo and Müller (1993)]:

$$\psi_1^\theta = \psi_{01} - s_{01}(\theta - \theta_0) - v_1\theta\left(\ln\frac{\theta}{\theta_0} - 1\right) - v_1\theta_0,$$

$$\psi_2^\theta = \psi_{02} - s_{02}(\theta - \theta_0) - v_2\theta\left(\ln\frac{\theta}{\theta_0} - 1\right) - v_2\theta_0. \tag{12}$$

Here $v_1 > 0$ and $v_2 > 0$ are specific heats, s_{01}, s_{02}, ψ_{01} and ψ_{02} are constants and θ_0 is a reference temperature. Note that in such a simplified case PT can be considered as growth of ε_0 from 0 to ε_{02} (ε_{02} is a constant for the given PT) which is accompanied by a jump in the thermal properties.

2.2. *The maximum principle for PT*

To determine all unknown parameters **b** (position, shape and orientation of nucleus, ε_1, ε_2 and so on) we use the postulate of realizability [Levitas (1995a, 1995c, 1996, 1997a, 1997b)]:

If, starting from the state without PT described by

$$F(\mathbf{b}^*) := \int_{V_n^*} (X(\mathbf{b}^*) - k(\mathbf{b}^*)) \, \mathrm{d}V_n < 0 \tag{13}$$

for all admissible PT parameters $\mathbf{b}^*$ in the course of variation of boundary data, the PT-condition (7) is fulfilled for the first time for some of parameters **b**, then nucleation will occur with this **b**.

If, in the course of variation of boundary data the criterion (7) is met for one or several **b**, then for arbitrary other $\mathbf{b}^*$ inequality (13) should be fulfilled, as in the opposite case for this $\mathbf{b}^*$ condition (7) had to be met before it was satisfied for **b**. Consequently, we obtain the maximum principle

$$\int_{V_n^*} (X(\mathbf{b}^*) - k(\mathbf{b}^*)) \, \mathrm{d}V_n < 0 = \int_{V_n} (X(\mathbf{b}) - k(\mathbf{b})) \, \mathrm{d}V_n \tag{14}$$

for determination of all unknown parameters **b**. Maximum principle (14) admits equivalent formulation:

$$F(\mathbf{b}^*) \to \max, \quad F(\mathbf{b}) = 0.$$

From principle (14) using eqn (8) we obtain

$$\int_{\varepsilon_1^*}^{\varepsilon_2^*}\int_{V_n^*}\boldsymbol{\sigma}^*:\mathrm{d}(\boldsymbol{\varepsilon}_e^*-\boldsymbol{\varepsilon}_t^*)\,\mathrm{d}V_n-\int_{V_n^*}\Delta\psi^*\,\mathrm{d}V_n-\int_{V_n^*}k^*\,\mathrm{d}V_n<0$$

$$=\int_{\varepsilon_1}^{\varepsilon_2}\int_{V_n}\boldsymbol{\sigma}:\mathrm{d}(\boldsymbol{\varepsilon}_e+\boldsymbol{\varepsilon}_t)\,\mathrm{d}V_n-\int_{V_n}\Delta\psi\,\mathrm{d}V_n-\int_{V_n}k\,\mathrm{d}V_n. \quad (15)$$

For particular case of PT criterion $(11)_1$ we have

$$\int_0^{\varepsilon_{02}}3\bar{\sigma}_0^*\,\mathrm{d}\varepsilon_0-\Delta\psi^\theta-k<0=\int_0^{\varepsilon_{02}}3\bar{\sigma}_0\,\mathrm{d}\varepsilon_0-\Delta\psi^\theta-k, \quad (16)$$

$$\bar{\sigma}_0^*=\frac{1}{V_n^*}\int_{V_n^*}\sigma_0^*\,\mathrm{d}V_n. \quad (17)$$

As only the work integral $\varphi:=\int_0^{\varepsilon_{02}}3\bar{\sigma}_0\,\mathrm{d}\varepsilon_0$ depends on the volume of nucleus V_n (its position and shape) and $\bar{\sigma}_0$ variation in it, then from maximum principle (16) it follows

$$\varphi(V_n^*,\bar{\sigma}_0^*)\to\max. \quad (18)$$

Note that the transformation strain $\varepsilon_0(\mathbf{r})$ ($\mathbf{r}$ is the position vector) grows from zero to ε_{02} in some V_n and in $V-V_n$ field $\varepsilon_0(\mathbf{r})$ is unchanged. The pressure $\bar{\sigma}_0$ is a functional of V_n and the process of $\varepsilon_0(\mathbf{r})$ variation in V_n.

Corresponding principles for points of coherent and noncoherent interfaces, based on principle (14), are given in detail [Levitas (1995a, 1995b, 1995c, 1996, 1997a, 1997b)]. The main essence of the maximum principle is that if only some dissipative process (plastic flow, PT) can occur, then it will occur, i.e. the first fulfilment of the necessary energetic condition is sufficient for the beginning of a dissipative process.

3. FORMULATION OF PROBLEM

Let us consider the problem formulation of martensitic PT in elastoplastic materials using the thermomechanical description of PT. For new (nucleus) and old (matrix) phases the standard isotropic elastic-perfectly-plastic model with von Mises yield condition is assumed, the elastic properties of both phases are the same and the transformation strain is volumetric. As an example of dilatational PT we can consider PT of graphite into diamond, of hexagonal nitride boron into cubic nitride boron, as well as PT in cesium and tin.

Here, PT will be considered as the thermomechanical process of growth of volumetric transformation strain from zero to final value ε_{02} in some volume V_n, which is accompanied by a change in thermal material properties. A set of equations includes the kinematic decomposition (2), the criterion of phase transition $(11)_1$, maximum principle (18) and the following relationships.

3.1. *Hooke's law*

$$\boldsymbol{\sigma}=\mathbf{E}:\boldsymbol{\varepsilon}_e=\lambda\boldsymbol{\varepsilon}_e:\mathbf{II}+2\mu\boldsymbol{\varepsilon}_e, \quad (19)$$

where λ and μ are the Lame coefficients.

3.2. *Von Mises yield condition*

$$f(\boldsymbol{\sigma})=\sigma_i-\sigma_y=0 \quad (20)$$

where $\sigma_i=(3/2\mathbf{s}:\mathbf{s})^{1/2}$ is the stress intensity, $\mathbf{s}=\mathrm{dev}\,\boldsymbol{\sigma}$ is the stress deviator and σ_y is the yield stress.

3.3. *The associated plastic flow rule*

$$\dot{\boldsymbol{\varepsilon}}_{\mathrm{p}} = \lambda \mathbf{s}; \quad \lambda \geqslant 0. \tag{21}$$

3.4. *Equilibrium equations for neglected body forces*

$$\nabla \cdot \boldsymbol{\sigma} = \mathbf{0}. \tag{22}$$

One of the mechanisms for getting a more advantageous stress variation in the transforming particle is related to the possibility of displacement discontinuities across the interface. We show a simple way of admitting noncoherence (sliding) and fracture [Levitas (1997a, 1997b)]. Three types of the interfaces between new and old phases are considered: coherent (with continuous displacements across the interface); noncoherent (with discontinuous tangential displacements across the interface); and the interface with fracture (with crack at the interface). We assume that PT and fracture (noncoherence) criteria are thermodynamically mutually independent and that these processes are coupled through the stress fields only. If, during the growth of ε_0 and variation of material thermal properties in nucleus, a chosen fracture criterion is met in some point of the interface, the crack appears or grows. If, in the same process, the noncoherence criterion is satisfied, we admit sliding in this point to a value where the criterion is violated. After completing the PT we check with the PT criterion whether PT is thermodynamically admissible. Consequently, the growing transformation strain $\varepsilon_0(\mathbf{r})$ generates the stresses which are necessary for the appearance of fracture or noncoherence, and fracture and noncoherence change the stress variation in the transforming particle. As the simplest fracture (noncoherence) criterion we assume that, if the normal to interface tensile (or shear) stress reaches some critical value, then the fracture (or sliding) in this point occurs. These conditions for a two-dimensional problem in a local coordinate system have the following form.

3.5. *Sliding condition at the interface (noncoherent interface)*

$$|\tau| < \tau_{\mathrm{s}} \Rightarrow \dot{\mathbf{u}}^2 - \dot{\mathbf{u}}^1 = 0, \tag{23}$$

$$|\tau| = \tau_{\mathrm{s}} \Rightarrow \dot{u}_{\mathrm{s}}^2 - \dot{u}_{\mathrm{s}}^1 \neq 0. \tag{24}$$

3.6. *Fracture condition at the interface*

$$|\sigma_{\mathrm{n}}| < \sigma_{\mathrm{c}} \Rightarrow \dot{\mathbf{u}}^2 - \dot{\mathbf{u}}^1 = 0, \tag{25}$$

$$|\sigma_{\mathrm{n}}| = \sigma_{\mathrm{c}} \Rightarrow \dot{\mathbf{u}}^2 - \dot{\mathbf{u}}^1 \neq 0, \quad \sigma_{\mathrm{n}} = \tau = 0, \tag{26}$$

where σ_n and τ are normal and tangential stresses at the interface, σ_{c} and τ_{s} are critical value of normal and shear stresses, $\dot{u}_{\mathrm{s}}$ is the tangential component of velocity at the interface and indices 1 and 2 identify those belonging to the matrix and the nucleus.

Thus, to determine the work integral φ in PT condition $(11)_1$, it is necessary to calculate the variation of local stress distributions as function of the growing transformation strain. For this purpose the standard elastoplastic contact problem with given volumetric transformation strain and contact conditions at the interface is solved numerically using FEM. Quadratic triangle displacement finite elements are used.

4. FINITE ELEMENT SOLUTION OF MODEL PROBLEMS

To determine the regularities of martensitic PT in elastoplastic materials using the PT criterion, we solve the simplest boundary-value problems. It is assumed that the dissipative threshold, k, is a function of temperature only. Then, at given temperature, k and $\Delta\psi^0$ are known, hence the value of the work integral φ (due to PT condition $(11)_1$) gives full information to evaluate the possibility of PT. For problem 4.1 the maximum principle (18) is not necessary, since the domain of nucleation is specified *a priori*, but we use the principle

to analyze the solution of the problem 4.2 and to define the positions of new nuclei for problem 4.3. The elastic properties are Young's modulus $E = 2 \cdot 10^5$ MPa and Poisson ratio $\mu = 0.3$.

4.1. *Nucleation of a spherical particle within a cylindrical sample*

Let us consider the axisymmetric formulation of the problem for a unit cell consisting of a spherical inclusion within a cylindrical matrix (Figs 1 and 2). Assume that at the given temperature and applied external axial pressure the spherical nucleus undergoes the dilatational martensitic transformation with $\varepsilon_{02} = -0.005$. The transformation of graphite particles, embedded in an iron matrix (cast iron), into diamond is a possible example. Below, we show how the temperature of PT at given external load for given place of PT region can be calculated. Because of symmetry, Fig. 1 shows a quarter of the unit cell of the composite, where X_1 is the horizontal axis of symmetry and X_2 is the axis of revolution, respectively. At first, a coherent interface between the particle and the matrix is assumed, i.e. the displacements are taken to be continuous across the interface. Then we consider noncoherent interface and interface with fracture (displacement discontinuities across the interface). In the general case for the unit cell the following formula is valid [e.g. Levitas (1992)]

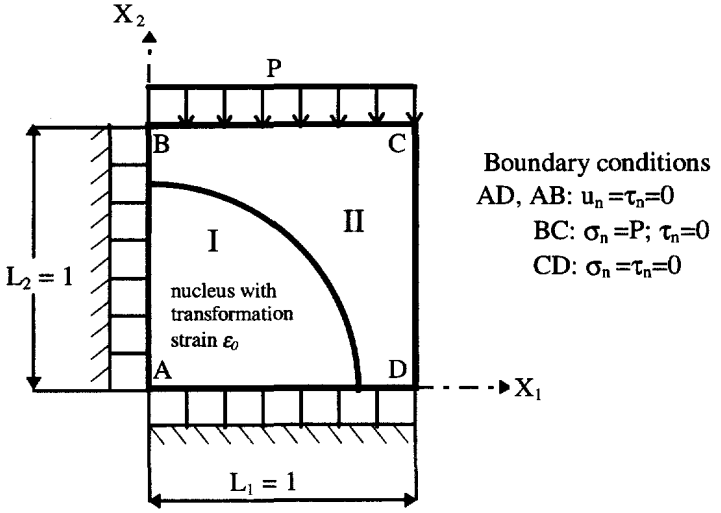

Fig. 1. A quarter of cross-section of the cylindrical matrix (II) with spherical nucleus (I).

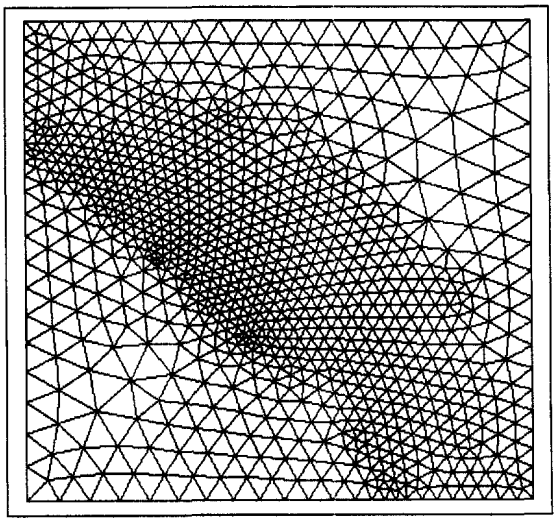

Fig. 2. Finite element mesh with refinement near the interface.

$$\boldsymbol{\sigma}(\mathbf{r}) = \mathbf{A}(\mathbf{r}) : \boldsymbol{\Sigma} + \boldsymbol{\sigma}_r(\mathbf{r}), \quad \boldsymbol{\Sigma} := \frac{1}{V}\int_S \mathbf{r}\boldsymbol{\sigma}\cdot\mathbf{n}\,dS = \frac{1}{V}\int_V \boldsymbol{\sigma}\,dV = \langle\boldsymbol{\sigma}\rangle, \tag{27}$$

where $\boldsymbol{\Sigma}$ is a mean (external) stress tensor, $\boldsymbol{\sigma}(\mathbf{r})$ is local stress tensor, $\boldsymbol{\sigma}_r(\mathbf{r})$ is the field of residual stresses at $\boldsymbol{\Sigma} = 0$ (i.e. $\langle\boldsymbol{\sigma}_r\rangle = 0$), $\mathbf{A}$ is the localization (concentration) fourth-order tensor and $\mathbf{n}$ is the external unit normal to the boundary S. In the case of homogeneous elastic properties $\mathbf{A}$ is an identity tensor, i.e.

$$\boldsymbol{\sigma}(\mathbf{r}) = \boldsymbol{\Sigma} + \boldsymbol{\sigma}_r(\mathbf{r}). \tag{28}$$

A superposition of an additional pure hydrostatic pressure in the above boundary-value problem does not influence the plastic strain and, consequently, the $\boldsymbol{\sigma}_r$. The additional hydrostatic pressure contributes additively to $\boldsymbol{\Sigma}$; according to eqn (28) it contributes also additively to $\boldsymbol{\sigma}$ and, consequently, to $\bar{\sigma}_0$ and can be taken into account analytically. That is why it is sufficient to consider macroscopically one-dimensional loading in out two-dimensional problem.

The following properties are used in the calculations: the yield stress for the matrix $\sigma_y^m = 2\cdot 10^2$ MPa and for the nucleus $\sigma_y^n = 0.46\cdot 10^2$ MPa. The following variation of yield limit $\tilde{\sigma}_y^n$ is assumed for nucleus during phase transition:

$$\tilde{\sigma}_y^n = \sigma_y^m + (\sigma_y^n - \sigma_y^m)\varepsilon_0/\varepsilon_{02}, \quad 0 \leqslant \varepsilon_0 \leqslant \varepsilon_{02}.$$

Volume fraction of nucleus is $c = 0.28$. The following boundary conditions are applied:

- along AB and AD boundaries $u_n = 0$, $\tau_n = 0$ (from symmetry condition);
- along CD boundary $\sigma_n = \tau_n = 0$ (free surface);
- along BC boundary $\sigma_n = P$, $\tau_n = 0$ (prescribed normal compressive stress P).

Here u_n is the normal displacement, τ_n is the tangential stress, σ_n is the normal stress.

The PT is simulated by growing of compressive strain ε_0 from 0 to -0.005 under fixed P (for matrix $\varepsilon_t = 0$). To obtain the value of work integral, φ, the elastoplastic contact problems are solved incrementally with a transformation strain increment $|\Delta\varepsilon_0| = 0.0005$. In a finite element code the transformation strain could be taken into account as a fictitious thermal strain. Five different values of P were considered, $P = 0$, 50, 100, 150 and 195 MPa.

It is necessary to note that for the problem under consideration the inverse problem has to be solved, i.e. the position and size of the PT region (nucleus) is specified *a priori* and then the condition for PT is determined. For example, if at a given external load the value of work integral, φ, is known from the calculations, then using scalar equation $(11)_1$ the temperature of PT can be obtained. The solution algorithm for the problem is briefly presented in Fig. 3.

4.1.1. *Fixed coherent interface (appearance of nucleus).* Let us consider the numerical results. The finite element mesh with the refinement near the interface, where large gradients of plastic strain occur, is shown in Fig. 2. Local fields of stresses, total and plastic deformations were determined. Isobands of hydrostatic pressure and accumulated plastic strain $q = \int(2/3\,d\boldsymbol{\varepsilon}_p : d\boldsymbol{\varepsilon}_p)^{1/2}$ are shown in Figs 4 and 5 at $P = 0$ and 150 (all results in Figs 4–8 are represented for elastic nucleus and elastoplastic matrix excluding curves 6 in Figs 6 and 7). At $P = 0$, the plastic region covers almost the whole cross-section of the matrix (excluding the upper right corner) and pressure is distributed nonuniformly both in the matrix (with positive and negative values) and in the nucleus (positive values). At $P = 150$, the plastic strain is concentrated near the interface, the maximal value of q is more than the three times the maximal value of q at $P = 0$. Such a concentration of plastic strain can lead to noncoherence at the interface. At the same time the pressure distribution is more uniform at $P = 150$ (positive in the nucleus, negative in the matrix). Figures 6 and 7 give the relationships between the averaged (over the nucleus) hydrostatic pressure, $\bar{\sigma}_0$, the work

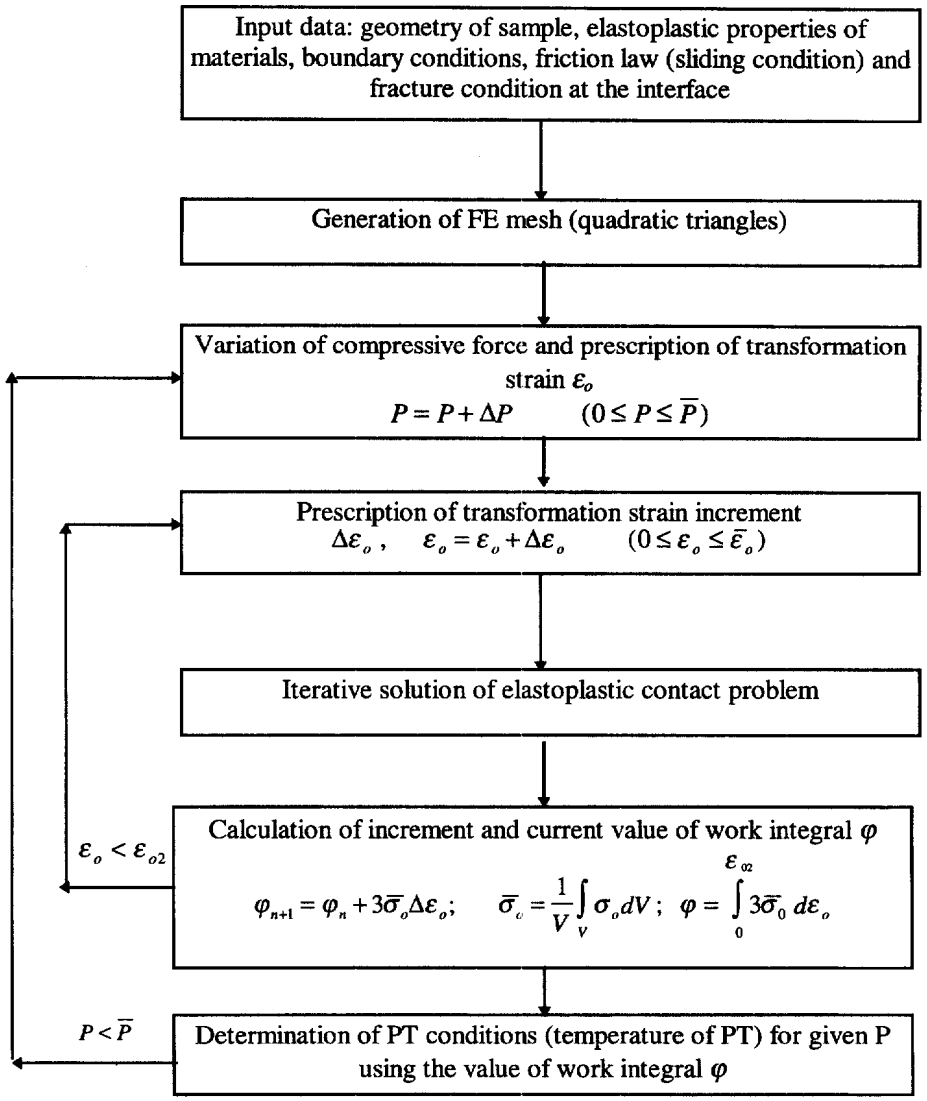

Fig. 3. Solution algorithm for phase transition (nucleation) in elastoplastic materials at uniaxial compression (coherent and noncoherent interface, interface with fracture).

integral, φ, and transformation volumetric strain, ε_0, for five different values of macroscopic axial stress, P. There is an evident saturation of values $\bar{\sigma}_0$ with the growth of ε_0 for each P, which is related to a limited plastic equilibrium state. The decrease of $\bar{\sigma}_0$ for elastoplastic nucleus (curve 6, Fig. 6) after $|\varepsilon_0| > 0.3\%$ is related to a decrease in the yield stress of the nucleus with the growth of transformation strain, ε_0. Practically linear dependence of φ from ε_0 at $|\varepsilon_0| > 0.1\%$, for each P allows the usage of a simple analytical approximation of the obtained numerical results.

Let us show how one can use the obtained numerical results to analyze the PT condition. It is evident that at $\sigma_y = 0$ and $P = 0$ we have $\bar{\sigma}_0 = 0$ and also assume that $k = 0$. Then the condition $(11)_1$ results in the ordinary PT criterion of chemical thermodynamics $\psi_2^\theta - \psi_1^\theta = 0$, which determines a phase equilibrium temperature θ_e. If in a thought experiment at $\sigma_y = 0$, $P = 0$, PT starts at temperature θ_s, then $k := \psi_2^\theta(\theta_s) - \psi_1^\theta(\theta_s)$. If k is a given function of θ then eqn $(11)_1$ determines the PT temperature. The value of the work integral, φ, at the given transformation volumetric strain, ε_0, and axial stress P is determined from Fig. 7. In particular, at $P = 0$, eqn $(11)_1$ should give an experimentally observed martensitic start temperature, M_s. If the PT temperature and transformation volumetric strain, ε_0, are given, then eqn $(11)_1$ determines the value of the work integral, φ, and axial stress, P, is determined from Fig. 7 (by interpolation). The work integral, φ, in most cases is negative,

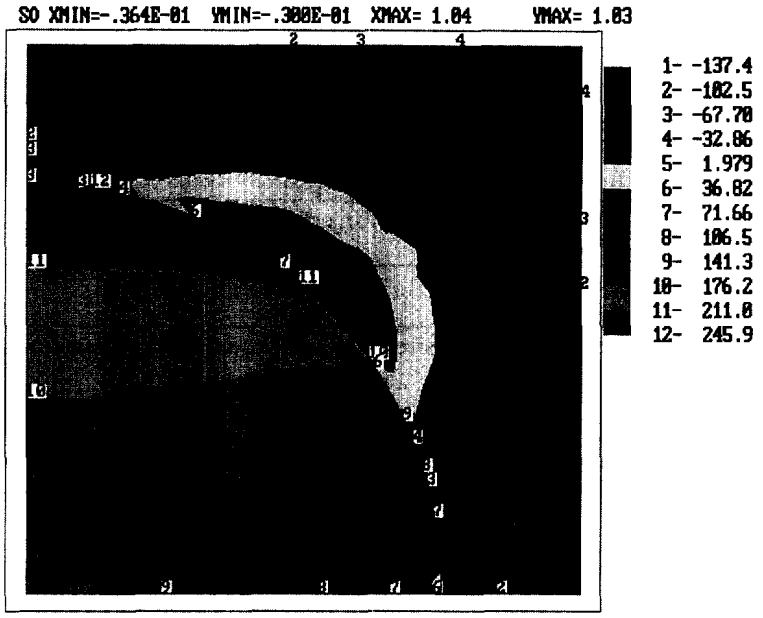

a

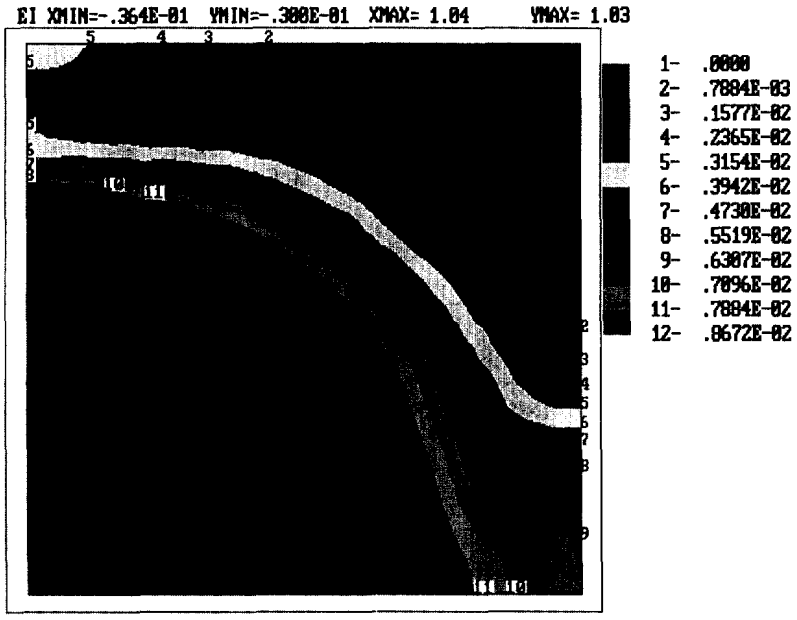

b

Fig. 4. Isobands of hydrostatic pressure (a) and accumulated plastic strain (b) distribution at volumetric transformation strain $|\varepsilon_{02}| = 0.005$ and $P = 0$ MPa (coherent interface).

i.e. mechanical work produces a negative effect (decreases the PT temperature) on the PT condition. The external compressive stress increases φ and the PT temperature (at $P = 195$, φ is positive). It is necessary to note that during transformation time (with growth of transformation strain) stresses are changed considerably, not only locally, but also the average value over the nucleus (Fig. 6).

4.1.2. *Cyclic appearance and disappearance of the coherent nucleus.* We investigate the problem of variation of the stress–strain state in an elastoplastic sample under cyclic appearance and disappearance of the new phase nucleus at given external stresses. The

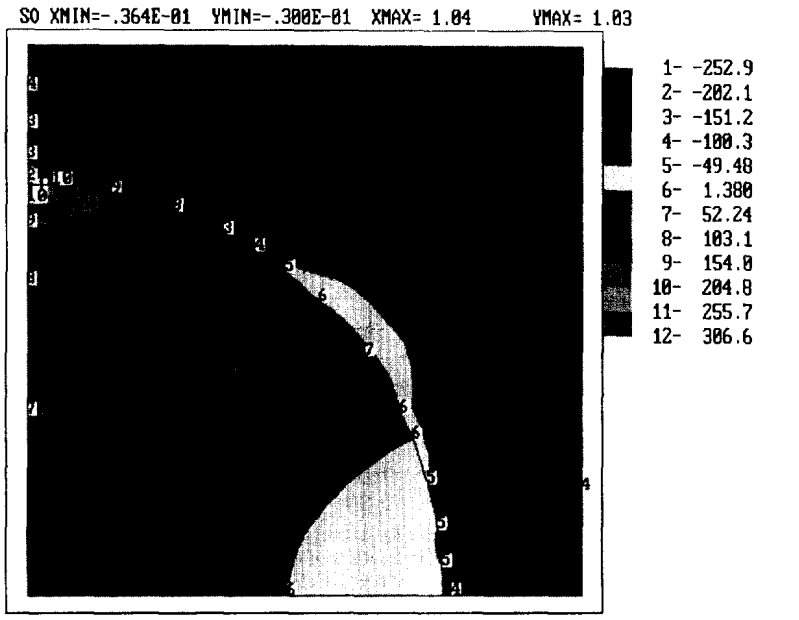

a

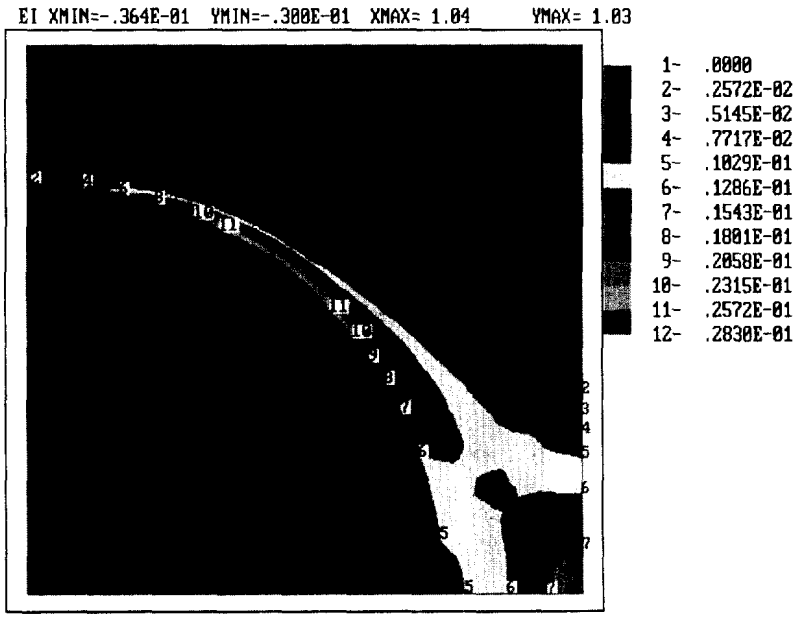

b

Fig. 5. Isobands of hydrostatic pressure (a) and accumulated plastic strain (b) distribution at volumetric transformation strain $|\varepsilon_{02}| = 0.005$ and $P = 150$ MPa (coherent interface).

formulation of the problem is the same as for previous one (4.1.1), but now the transformation strain in the spherical particle increases at first until $\varepsilon_0 = -0.005$, then decreases to zero (first cycle). Such cycles (due to cyclic temperature variation) are repeated. The following assumptions are introduced: the interface is coherent and the nucleus is elastic (for the problem under consideration, calculated stress intensity in the nucleus after reverse PT is less than the yield stress of the matrix, i.e. the nucleus is also elastic at reverse PT). In Fig. 8 the relationship between the axial plastic strain, $\bar{\varepsilon}_2^p$, (a) averaged over the unit cell and variation of hydrostatic pressure, $\bar{\sigma}_0$ (b) averaged over the nucleus, for five cycles of appearance and disappearance of the new phase nucleus, is presented ($P = 50$). At the same elastic properties of the matrix and nucleus, the value $\bar{\varepsilon}_2^p$ is the macroscopic axial plastic

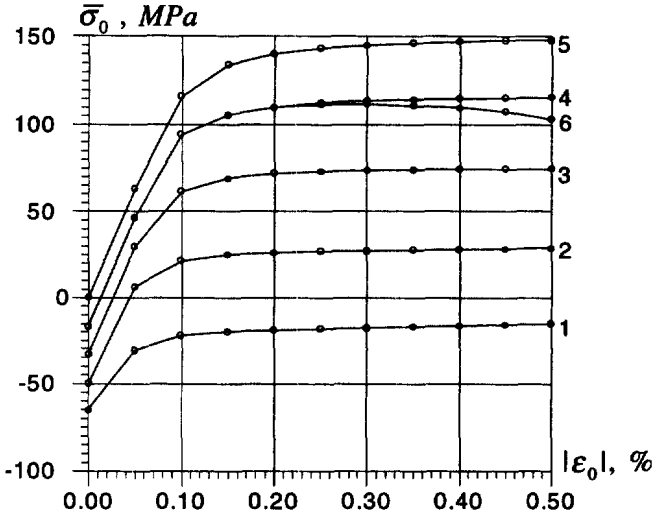

Fig. 6. Relationship between hydrostatic pressure $\bar{\sigma}_0$, averaged over the nucleus and transformation volumetric strain ε_0. 1,2,3,4(6),5 correspond to the values of compressive force $P = 195; 150; 100; 50; 0$. 1–5 are for elastic nucleus, 6 is for elastoplastic nucleus.

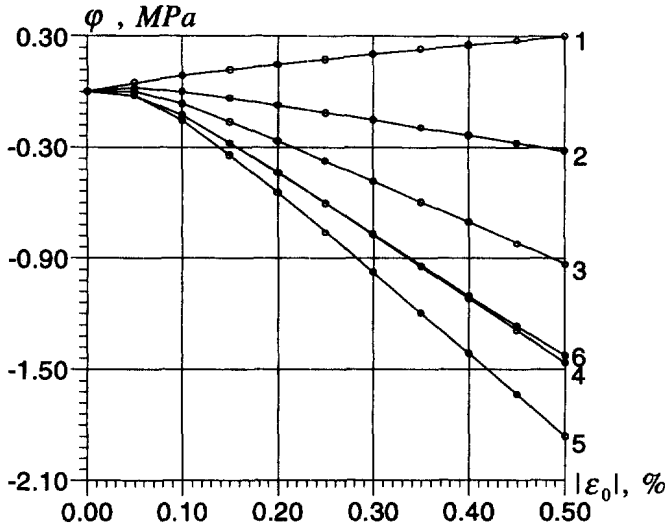

Fig. 7. Relationship between the work integral φ and transformation volumetric strain ε_0. (1,2,3,4(6),5 correspond to the values of compressive force $P = 195; 150; 100; 50; 0$. 1–5 are for elastic nucleus, 6 is for elastoplastic nucleus).

strain. It follows that increments of the macroscopic axial plastic strain per cycle, beginning from the second cycle, are almost the same and it is possible to predict the material behavior at cyclic PT using only the first two cycles. This problem models the well-known TRIP phenomena due to Greenwood–Jonson effect, when at relatively small external compressive stresses (much less than yield stresses) it is possible to obtain a very large value of macroscopic plastic strains due to PT [Mitter (1987); Padmanabhan and Dabies (1980)].

Now the work integral, φ, is investigated. Beginning from the second cycle for direct PT $\varphi_d = -0.63$ MPa and for reverse PT $\varphi_r = -1.47$ MPa. The corresponding temperature of direct θ_d and reverse θ_r PT can be determined from the PT condition $(11)_1$ as

$$\varphi_d - \Delta\psi^\theta(\theta_d) = k_d, \tag{29}$$

$$\varphi_r + \Delta\psi^\theta(\theta_r) = k_r, \tag{30}$$

where k_d and k_r are the values of dissipation due to the direct and reverse PT. From eqns

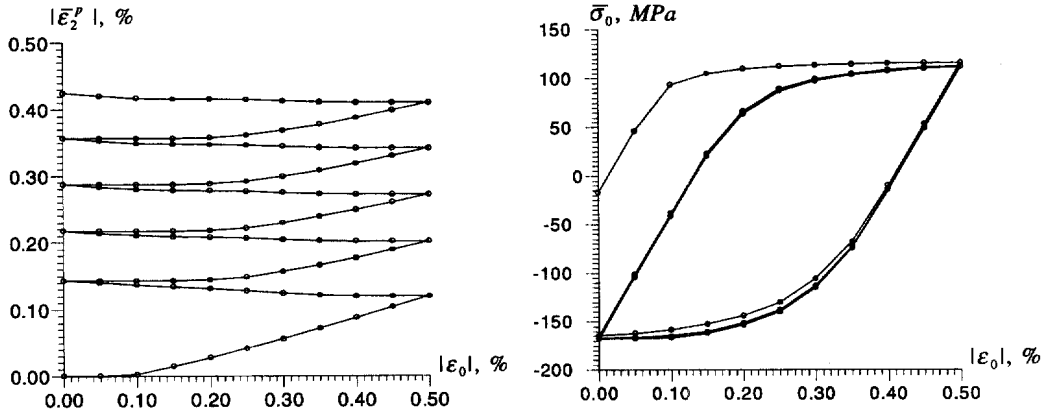

a b

Fig. 8. Relationship between axial plastic strain $\bar{\varepsilon}_2^p$ (a), averaged over the unit cell, and variation of hydrostatic pressure $\bar{\sigma}_0$ (b), averaged over the nucleus, for five cycles of appearance and disappearance of new phase nucleus ($P = 50$ MPa).

(29) and (30), temperature hysteresis, $\theta_d - \theta_r$, can be calculated easily. For example, if dissipation, due to PT itself, equals zero ($k_d = k_r = 0$), temperature hysteresis is not zero ($\theta_d \neq \theta_r$) due to $\varphi_d + \varphi_r = -2.1 \neq 0$ (i.e. due to plastic deformation, which is allowed for at the calculation of the work integral, φ).

4.1.3. *Fixed noncoherent interface (sliding).* Let us investigate the influence of noncoherence of the interface on the PT condition. The same boundary-value problem as for the coherent interface (the problem 4.1.1) is considered. To evaluate the range of sliding influence the simplest friction conditions (23) and (24) with $\tau_s = 0$ (this is the limit case, another limit case is coherent interface) and intermediate values of critical shear stress $\tau_s = 40$ and 100 are assumed (maximum possible value $\tau_{s\max} = (1/3)^{1/2}\sigma_y = 115$ MPa). Isobands of displacements, hydrostatic pressure and accumulated plastic strain distribution at $P = 150$ MPa (noncoherent interface with critical shear stress $\tau_s = 40$ MPa) are presented in Figs 9 and 10. Between points A and B the sliding zone is formed. The biggest jump of displacements at the interface (different shades across interface correspond to the jump of displacement) has a vertical component of displacement in the middle of the sliding zone, between points A and B [Fig. 9(b)]. Near this zone there is pressure concentration from the side of the nucleus [Fig. 10(a)]. The values of pressure in the nucleus is changed from negative to positive. Plastic strains are concentrated in the matrix near the horizontal axis X [Fig. 10(b)], with approximately the same maximum value as for coherent interface (but in another place). Figures 11 and 12 give the relationships between the averaged (over the nucleus) hydrostatic pressure, $\bar{\sigma}_0$, the work integral, φ, and transformation volumetric strain, ε_0, for different values of critical stress, τ_s (curves 1–4). As can be seen from Figs 11 and 12, noncoherence affects considerably the stress state of a sample and encourages the PT, because the value of work integral, φ (and, consequently, driving force $\bar{X}$ for PT) is much bigger for the noncoherent interface than for the coherent one.

4.1.4. *Fixed interface with fracture.* For the noncoherent interface, jumps of tangential displacement are permitted only, and for the interface with fracture jumps of normal displacement can occur, which means the crack appearance. Solving, incrementally, the elastoplastic contact problem with fracture conditions (25) and (26) and $\sigma_c = 50$ MPa, the progress of the crack at the interface and the variation of local stress fields are determined as functions of the growing transformation strain. Isobands of displacements, hydrostatic pressure and accumulated plastic strain distribution at $P = 150$ MPa with critical normal stress $\sigma_c = 50$ MPa are presented in Figs 13 and 14. The final position of the crack is between points A and B (Figs 13 and 14). The distribution of vertical displacements is similar to the case of the noncoherent interface, but the maximum positive value of horizontal

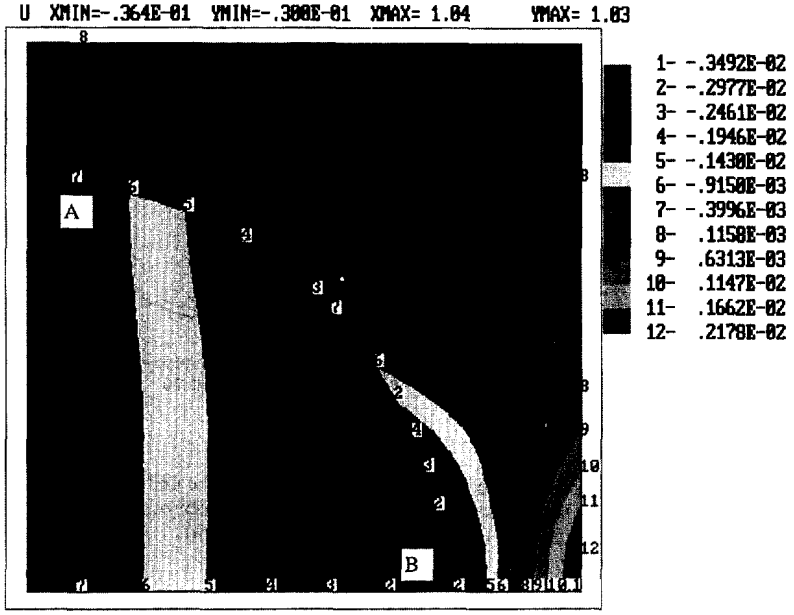

a

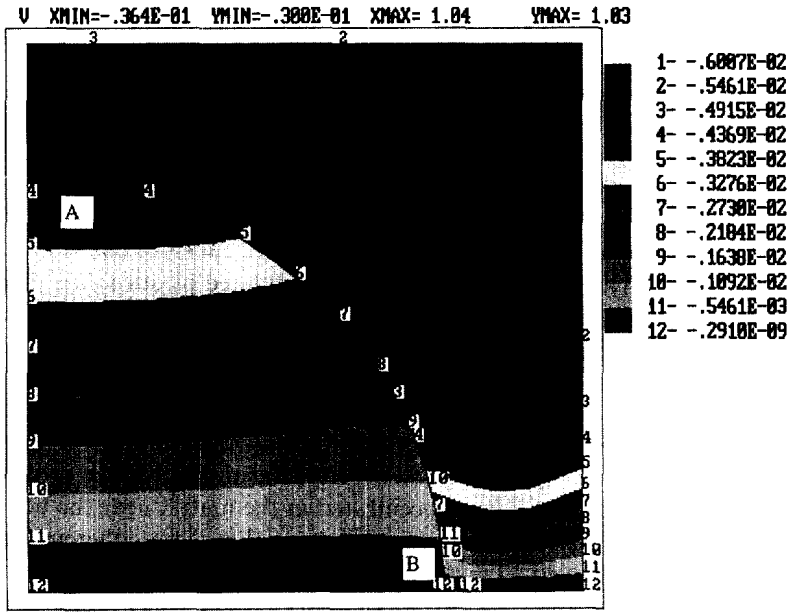

b

Fig. 9. Isobands of horizontal (a) and vertical (b) displacement distribution (mm) at volumetric transformation strain $|\varepsilon_{02}| = 0.005$ and $P = 150$ MPa (noncoherent interface with maximum shear stress $\tau_s = 40$ MPa). AB is the sliding zone.

displacements is considerably bigger than for the case of the noncoherent interface (more than two times). The pressure distributions for the interface with fracture and the noncoherent interface differ considerably both qualitatively and quantatively [Figs 10(a) and 14(a)]. Near the crack tips (points *A* and *B*) the strong concentration of plastic strains occurs [Fig. 14(b)]. Curve 5 in Figs 11 and 12 shows the effect of fracture with the growth of transformation strain. Until $|\varepsilon_0| = 0.1\%$, the interface is coherent. Then, with the growth of transformation strain, ε_0, a large crack appears along the greater part of the interface and then for $|\varepsilon_0| > 0.15\%$, a small growth of the crack occurs with the growth of ε_0. Small oscillations of curve 5 in Fig. 11 at $|\varepsilon_0| > 0.35\%$ are related to problem discretization: for

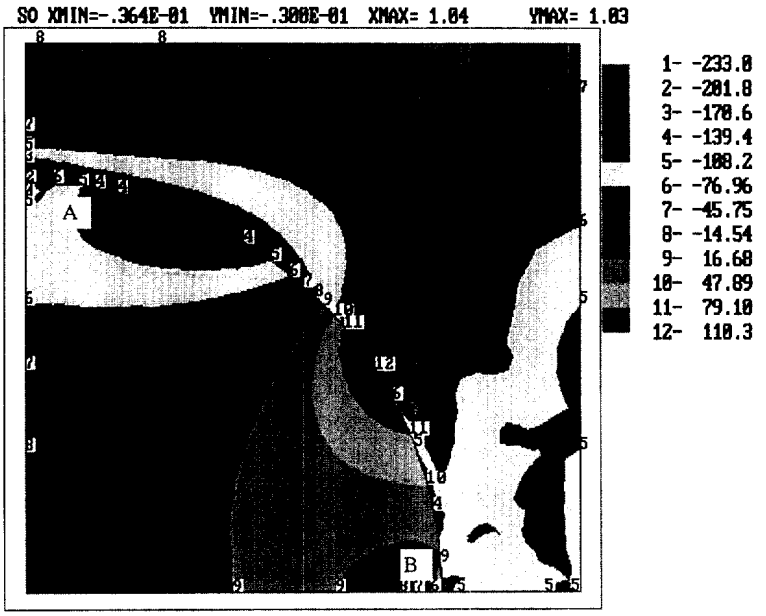

a

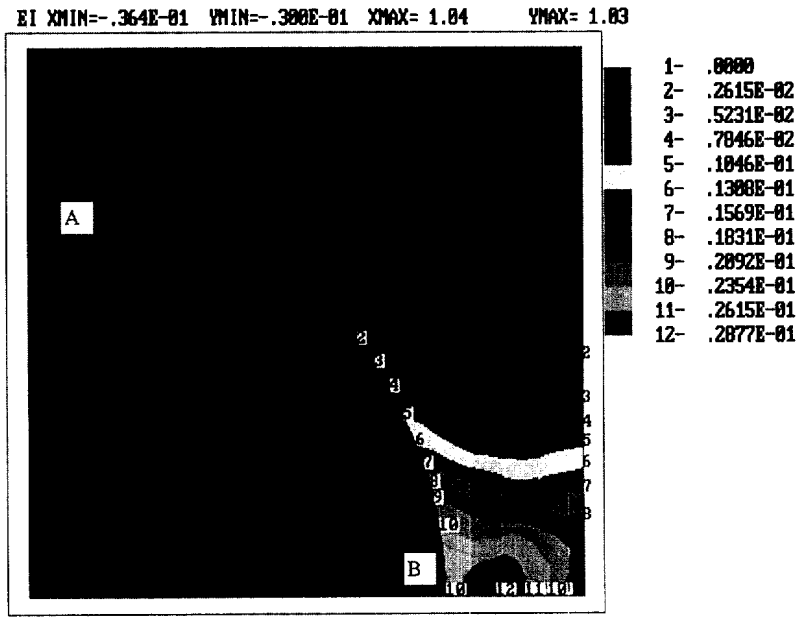

b

Fig. 10. Isobands of hydrostatic pressure (a) and accumulated plastic strain (b) distribution at volumetric transformation strain $|\varepsilon_{02}| = 0.005$ and $P = 150$ MPa (noncoherent interface with maximum shear stress $\tau_s = 40$ MPa). AB is the sliding zone.

a loading step at $|\varepsilon_0| = 0.35\%$, the crack does not progress; and for a loading step at $|\varepsilon_0| > 0.40\%$, the crack tip is shifted along the length of a finite element and so on. Fracture (as well as sliding) at the interface encourages PT, because the value of the work integral, φ, is much bigger for the interface with fracture than for the coherent one.

4.2. *The progress of PT (layer by layer) in a cylindrical sample (moving coherent and noncoherent interface)*

Above, the PT with the fixed interface was considered. Now we examine the case of moving the coherent and noncoherent interfaces in a cylindrical sample to get regularities

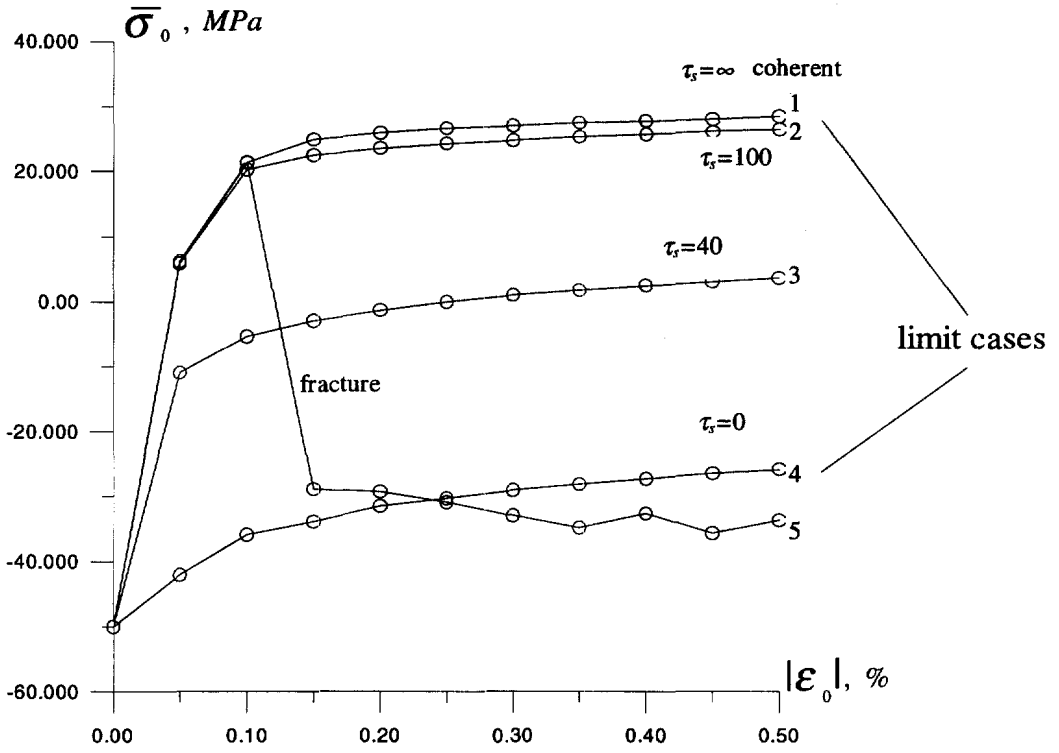

Fig. 11. Relationships between hydrostatic pressure $\bar{\sigma}_0$, averaged over the nucleus and transformation volumetric strain ε_0 at $P = 150$ Mpa. 1—coherent interface; 2,3,4—noncoherent interface with maximum critical shear stresses $\tau_s = 100$; 40; 0 MPa, respectively; 5—with fracture at the interface, maximum normal stress $\sigma_c = 50$ MPa.

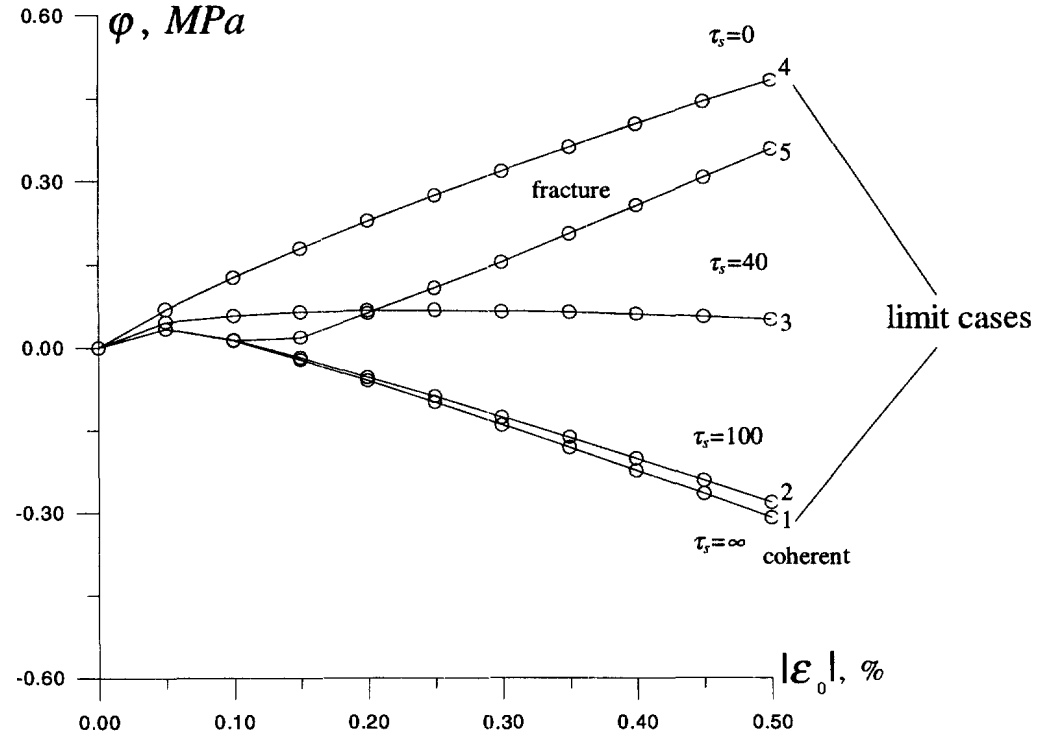

Fig. 12. Relationships between the work integral φ (mechanical part of PT driving force) and transformation volumetric strain ε_0 at $P = 150$ MPa. 1—coherent interface; 2,3,4—noncoherent interface with maximum critical shear stresses $\tau_s = 100$; 40; 0 MPa, respectively; 5—with fracture at the interface, maximum normal stress $\sigma_c = 50$ MPa.

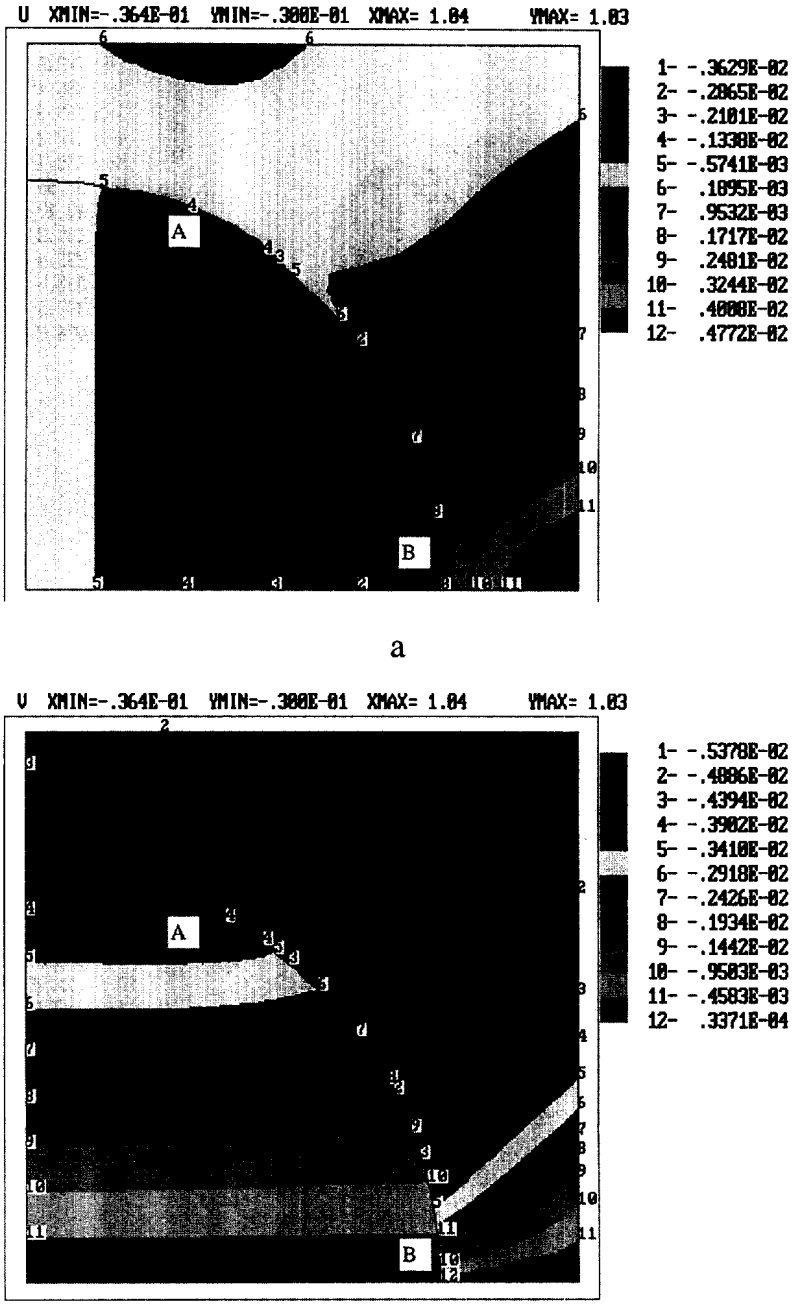

Fig. 13. Isobands of horizontal (a) and vertical (b) displacement distribution (mm) at volumetric transformation strain $|\varepsilon_{02}| = 0.005$ and $P = 150$ MPa (with the fracture on the interface, maximum normal stress $\sigma_c = 50$ MPa). AB is the fracture zone.

of the PT progress, i.e. to study the influence of internal stresses, plastic deformation and noncoherence due to the preceding PT on the conditions of subsequent PT. Figures 15 and 16 show the cross-section and the mesh of a cylindrical sample divided into layers. The following boundary conditions are applied:

- along CD and DE boundaries $u_n = 0$, $\tau_n = 0$;
- along EF boundary $\sigma_n = \tau_n = 0$ (free surface);
- along CF boundary $\sigma_n = P = 100$, $\tau_n = 0$ (prescribed compressive stress P).

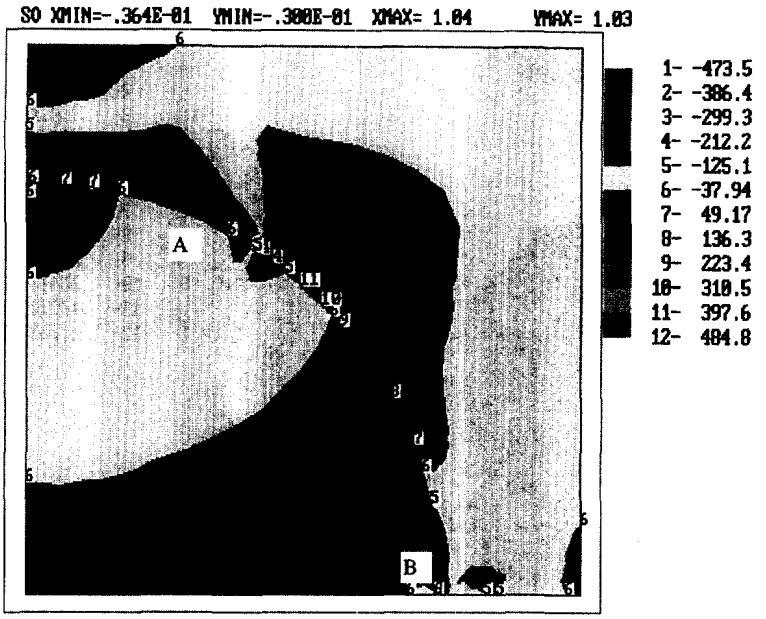

a

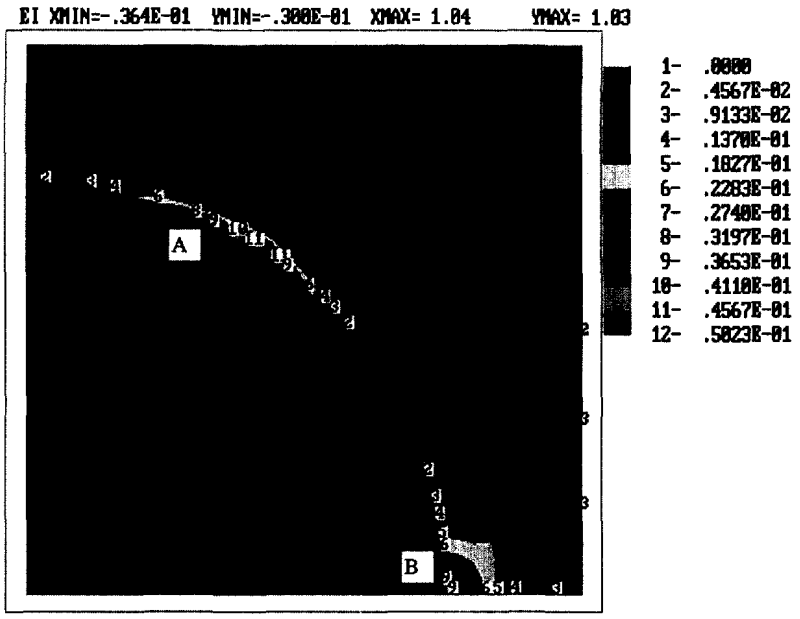

b

Fig. 14. Isobands of hydrostatic pressure (a) and accumulated plastic strain (b) distribution at volumetric transformation strain $|\varepsilon_{02}| = 0.005$ and $P = 150$ MPa (with the fracture at the interface, maximum normal stress $\sigma_c = 50$ MPa). AB is the fracture zone.

The yield stress for the matrix is $\sigma_y^m = 4.5 \cdot 10^2$ MPa. The new phase is assumed to be elastic. The moving interface is modeled as a different position of fixed interface, for which PT is described in the same ways as for problems 4.1.1–4.1.3.

For this example, we also consider the inverse problem, i.e. we specify *a priori* the sequence of the positions of the interface (and the region where PT occurs) during the time, and for every interface position the PT condition is calculated, as for previous problems. For the problem under consideration, we specify five different sequential positions of the interface. At the beginning, PT occurs in the first layer with interface A_1B_1; then PT occurs in the second layer with interface A_2B_2 and so on. The interface between the layer of the

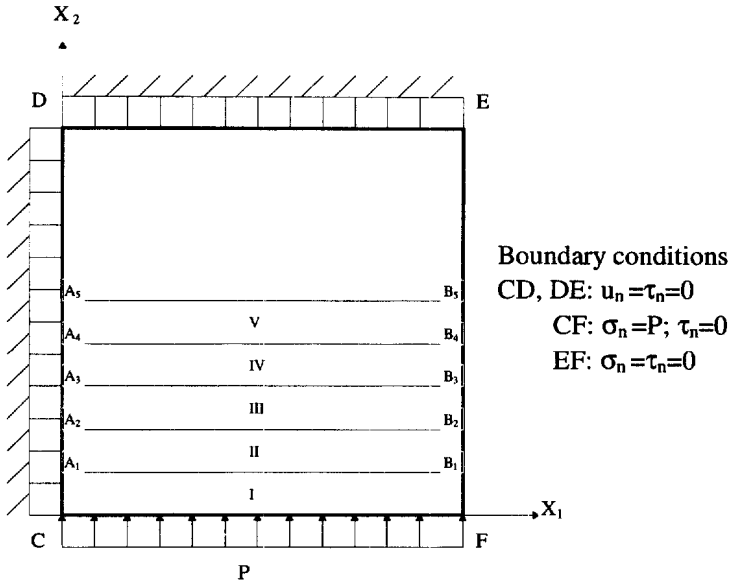

Fig. 15. A half of cross-section of a cylindrical sample. A_1B_1, A_2B_2, A_3B_3, A_4B_4, A_5B_5 are the positions of the interface at different time instants (I, II, III, IV, V are the regions where PT occurs after corresponding displacement of the interface). X_2 is axis of rotation.

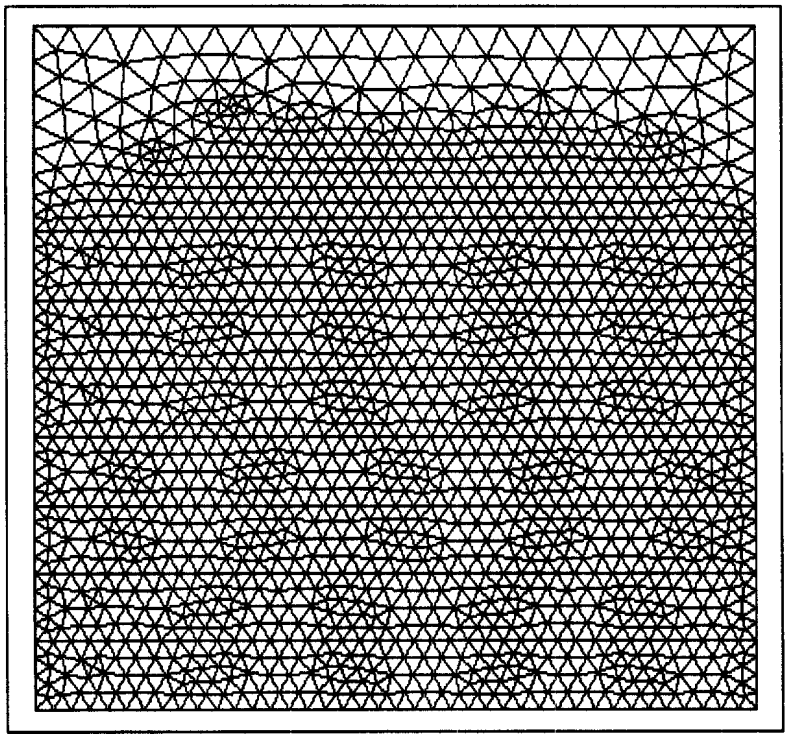

Fig. 16. Finite element mesh with refinement in transforming layers.

new phase and the matrix can be coherent or noncoherent with a critical value of shear stress at the interface $\tau_s = 200$. After finishing the PT in the layer, the displacement discontinuities at the layer interface do not change anymore. In particular, the interface between the layer of new phase and the layer, where PT is still occurring, can be treated as the coherent one because additional discontinuities do not occur.

The PT, in a layer, is simulated by the growing of the compressive transformation strain, ε_0, from 0 to -0.01 with the increment $|\varepsilon_0| = 0.002$, under fixed P. The algorithm of solving the problem is the same as for problem 4.1.3, but after determining the PT condition for one layer, calculations go on to the next layer with a new position of the interface. The

local stresses of the previous solution are used as initial data for calculation of the PT condition of subsequent layers.

4.2.1. *The coherent interface (elastic matrix).* Figure 17 shows the variation of hydrostatic pressure, $\bar{\sigma}_0$, (a) averaged over the layer and variation of the work integral, φ, (b) for the ith layer in the course of PT in the ith layer, $i = \mathrm{I}, \mathrm{II}, \mathrm{III}, \mathrm{IV}, \mathrm{V}$. We have a linear variation of $\bar{\sigma}_0$ with the growth of the PT strain for every layer (due to linear elastic problem). PT for the coherent interface at $k = \text{const}$ is unstable (according to the maximum principle (18)), i.e. if PT occurs in the first layer, then at the same temperature and external stresses PT should occur in all the remaining layers, because the value of work integral, φ (and, hence, driving forces $\bar{X}$) at transformation strain $|\varepsilon_0| = 0.01$, is larger for the remaining layers than for the first one. Consequently, to describe the stable phase equilibrium we should assume heterogeneous k distribution or assume that k grows with increasing total volume fraction c of a new phase in a specimen. As a final value of φ is almost constant, starting with the third layer, the interface can be arrested in position A_3B_3 or A_4B_4.

4.2.2. *The noncoherent interface (elastic and elastoplastic matrix).* Let us consider the noncoherent interface. Figure 18 (elastic matrix) shows us isobands of radial displacements distribution at different values of transformation strain in course of PT of the layer $I(a-e)$ and at the motion of the interface until the middle of a sample (f). With the growth of transformation strain the growth of the sliding zone takes place (different shades across the interface correspond to the jump of displacements). The biggest sliding zone at the interface takes place for PT in the first layer. For subsequent positions of the interface the sliding zone decreases. The axial stress [Fig. 19(a)] is continuous with large regions of positive and negative values. The hydrostatic pressure [Fig. 19(b)] distribution is discontinuous across the interface and has a complicated character with a variation of the values from negative to positive within every layer. Figure 20 shows the variation of hydrostatic pressure (a) averaged over the layer and the variation of the work integral, φ; (b) for the ith layer in the course of PT in the ith layer, $i = \mathrm{I}, \mathrm{II}, \mathrm{III}, \mathrm{IV}, \mathrm{V}$. For elastic material the nonlinear change of $\bar{\sigma}_0$, with the growth of PT strain within the layer (due to variation of sliding zone), takes place [curve 1, Fig. 20(a)]. More linear character of curves 2–5 in the Fig. 20(a) is connected with the influence of the region where PT has already occurred (because at the interface, between the layer of new phase and the layer where PT is still occurring, there are no additional displacement discontinuities).

Comparison of Figs 17 and 19 shows that the noncoherence stimulates significantly the PT condition in the first layer (φ increases). The PT condition in the second layer for the noncoherent interface is worse than for the coherent interface, but a little bit better than for the first layer of the noncoherent interface. That is why at $k = \text{const}$, or slightly growing $k(c)$, the noncoherent PT in the second layer can occur, at once, after the PT in the first layer at the same external condition (temperature or loading). The value, φ, for the noncoherent PT in the third layer is smaller than for first and second layers and much smaller than for the third layer for the coherent PT. If the value $k(c)$ is large enough to stop the coherent interface motion at fixed external parameters in position A_2B_2, A_3B_3 or A_4B_4 ($\varphi \simeq 0$ Mpa), then it is necessary to change external parameters very significantly to shift the noncoherent interface ($\varphi \simeq -12$ MPa), but at such a change of external parameters, the PT can occur in other places of a sample.

For example, we have investigated the problem for another sequence of the PT in layers for the coherent and noncoherent interfaces. Two cases are considered: (a) after the PT in the first layer, the PT occurs in the second layer: (b) after the PT in the first layer, the PT occurs in the third layer. For the coherent interface the work integral, φ, in the transforming layer is bigger for case (a) than for case (b). For the noncoherent interface at some small value of critical shear stress, τ_s, the value of work integral, φ, for the transforming layer was bigger for case (b) than for case (a), i.e. the PT can be more profitable in the layer which is not in contact with the transformed one.

Now we consider this problem with $P = 0$ and $\tau_s = 0$ (limit case). Then for any layer, if it is not in contact with the transformed layer (interface between matrix and transforming

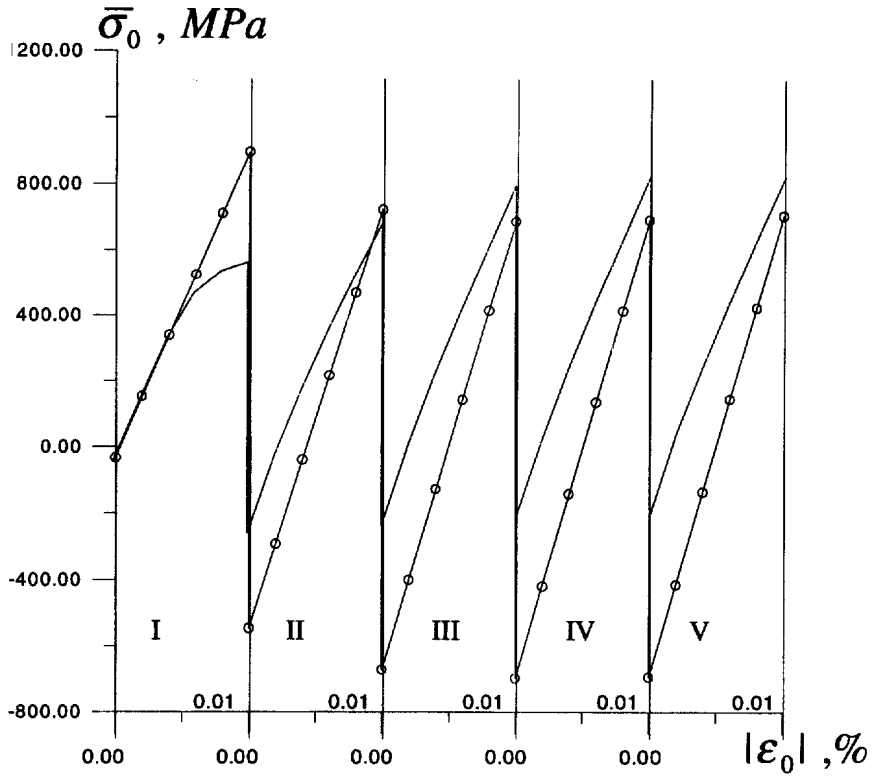

a

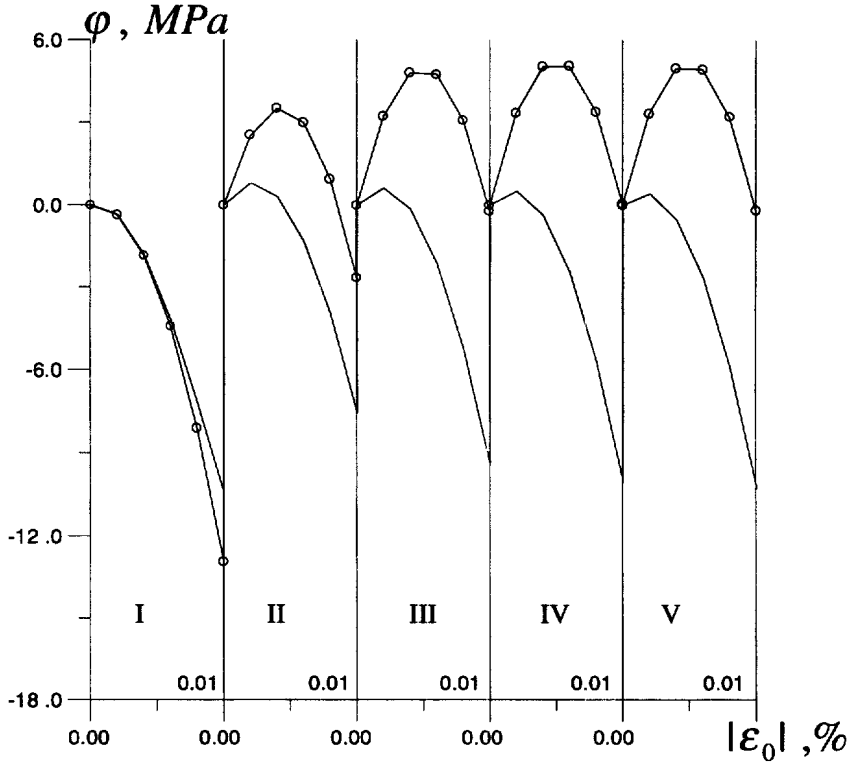

b

Fig. 17. Variation of hydrostatic pressure $\bar{\sigma}_0$ (a) averaged over the layer and variation of the work integral φ (b) for the ith layer in the course of PT in the ith layer for moving coherent interface and elastic matrix, i = I,II,III,IV.

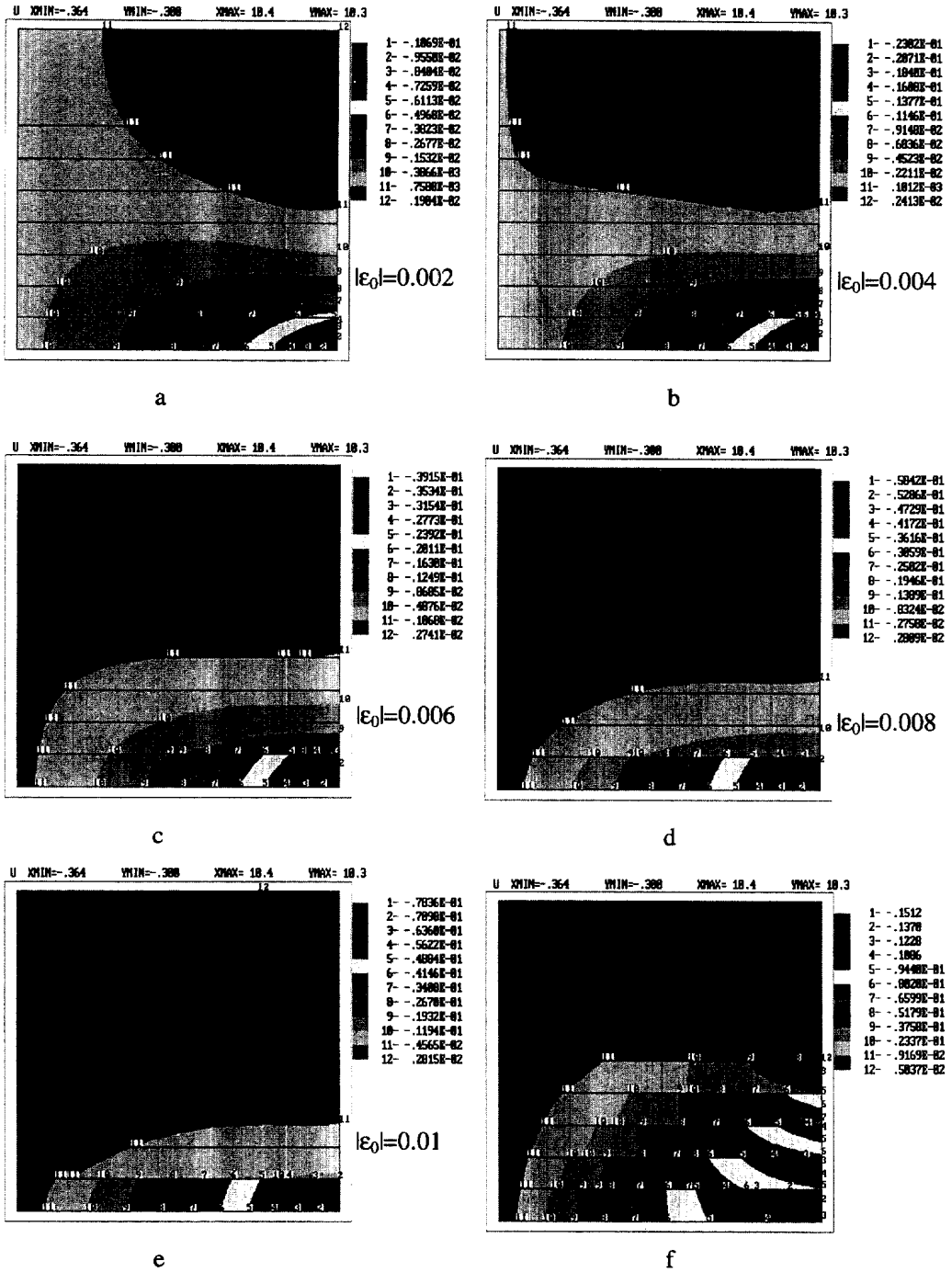

Fig. 18. Isobands of radial displacement distribution (mm) for noncoherent interface at different values of transformation strain in course of PT within the first layer (a–e) and at the interface motion until the middle of a sample (f).

layer is noncoherent), the work integral, φ, is zero (because stresses are zero due to $\tau_s = 0$), but if the transforming layer is in contact with the transformed one (interface between these layers is coherent according to the problem formulation), the work integral, φ, is negative (because of the jump of negative transformation strain across the interface we have positive average pressure in the transforming layer). Thus, noncoherence relaxes the stresses and can enforce the complicated kinetics of new phase, i.e. varying critical shear stress, τ_s, can change the kinetics of PT.

These results explain known experimental facts, for example, that the noncoherent interface has a low mobility or cannot move at all. The reason for the decreasing value, φ,

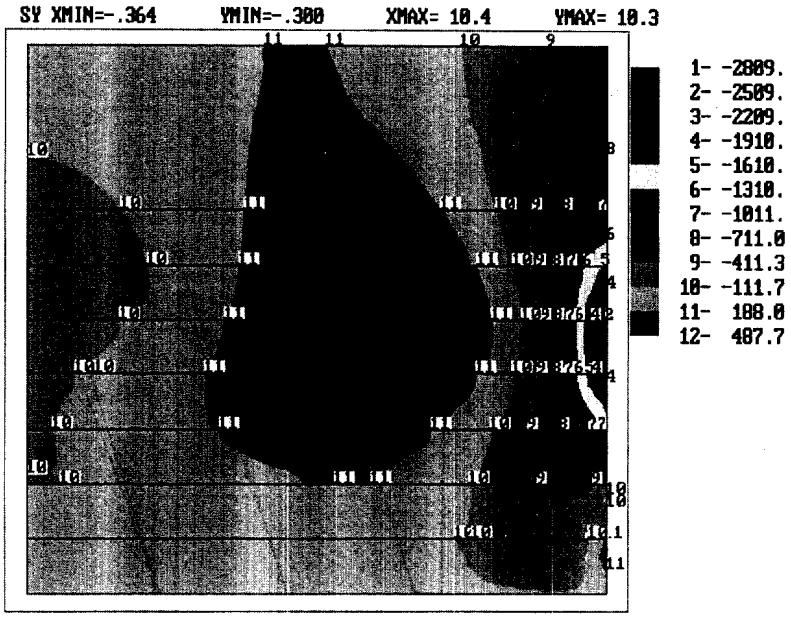

a

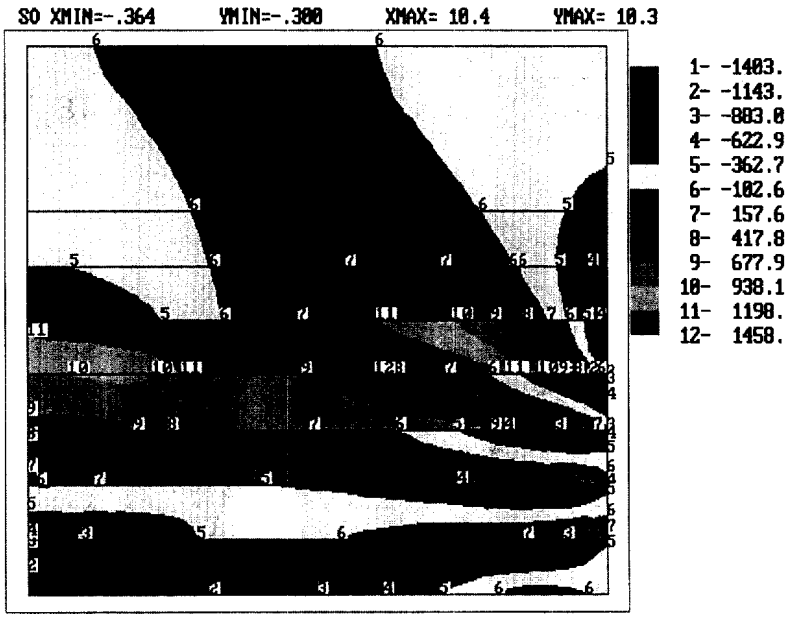

b

Fig. 19. Isobands of axial stresses (a) and hydrostatic pressure (b) distribution at the interface motion until the middle of a sample.

and for moving the noncoherent interface is the change of internal stresses. So, initial negative internal stresses in the transforming layer (due to the transformation strain in the previous layer), which promote the PT, decrease (absolute value) considerably due to stress relaxation during the sliding at the interface [compare initial values $\bar{\sigma}_0$ for the layers in Figs 17(a) and 20(a)].

The slight difference of results for elastic and elastoplastic matrices (difference holds only seen for PT in 3–5 layers, Fig. 20) is explained by the fact that with chosen mechanical properties, with values of transformation strain and with critical shear stress, sliding at the interface is more important than plastic deformation. Thus, for both fixed and moving interface, the noncoherence changes PT conditions, considerably.

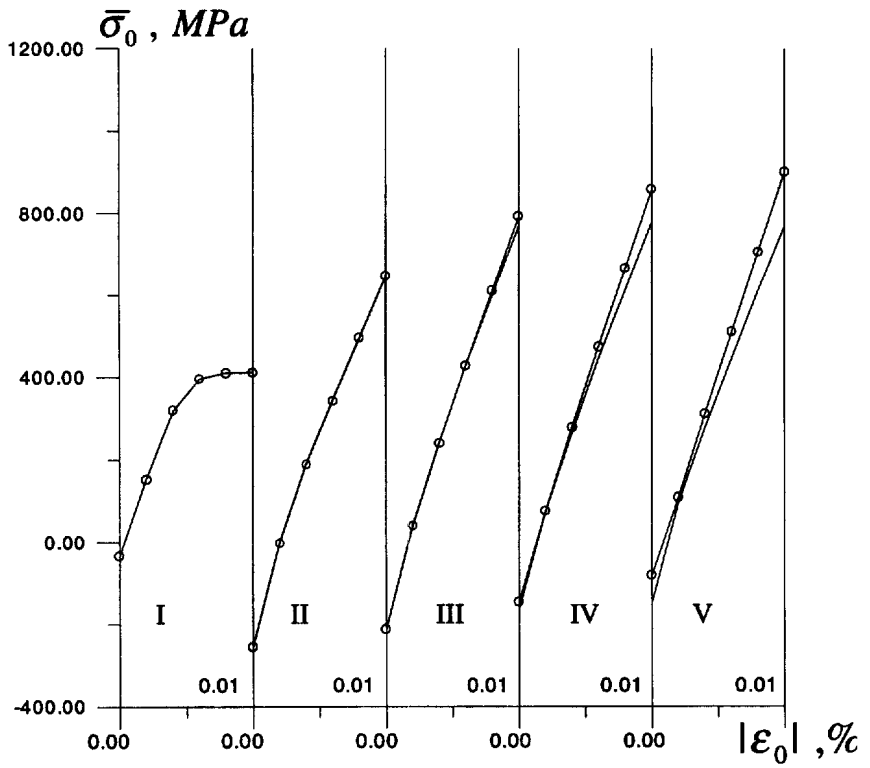

Fig. 20. Variation of hydrostatic pressure $\bar{\sigma}_0$ (a) averaged over the layer and variation of the work integral (b) for the ith layer in the course of PT in the ith layer for moving noncoherent interface, i = I,II,III,IV,V. (○—for elastic matrix; ——for elastoplastic matrix).

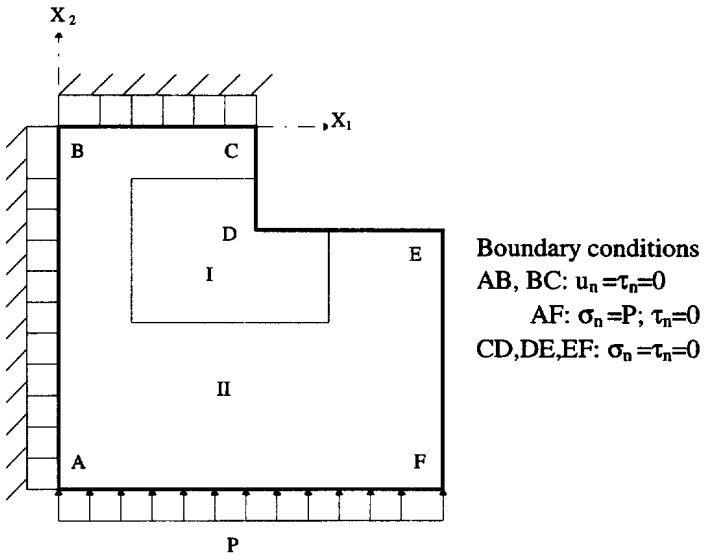

Fig. 21. A quarter of cross-section of the cylindrical sample with notch. I is the admitted PT region.

4.3. *Progress of PT region*

Let us consider the axisymmetric problem of PT in a sample with a notch under the external compressive load P (Figs 21 and 22). The sample with a notch is used to obtain an initial stress concentration before the PT. The following boundary conditions are applied:

- along AB and BC boundaries $u_n = 0$, $\tau_n = 0$ (from symmetry condition);
- along CD, DE and EF boundaries $\sigma_n = \tau_n = 0$ (free surface);
- along AF boundary $\sigma_n = P = 100$, $\tau_n = 0$ (prescribed compressive stress P).

The yield stress for the matrix is $\sigma_y^m = 5 \cdot 10^2$ Mpa. The nucleus is assumed to be elastic and the transformation strain is $\varepsilon_{02} = -0.005$.

Now we do not specify, *a priori*, the region where the PT will occur, but determine the PT region. To decrease the calculation expenditure, we only specify in advance the region admitted for PT (active set), where PT can occur (if it is impossible we should consider the whole domain as admitted for PT). The following assumption is posed for calculation: PT occurs at any time instant in one finite element (FE) only. For this state, the whole deformation process of PT in the FE has to be computed. Every FE is considered as a possible new nucleus. To choose the FE, where PT can occur, we should find the FE for which the functional φ has a maximum value (see (18)). Only after finishing the PT in one element can the PT start in another one. In the sequel, the solution algorithm is described for this problem.

(1) Specify input data: geometry of sample, elastoplastic properties of materials, boundary conditions and FE mesh.
(2) Prescribe the admitted PT region (active set).
(3) Check all the elements in the admitted PT region, on the possibility of PT. For this purpose we suppose that PT occurs in one element, then solve the elastoplastic problem with a specified transformation strain in this element and calculate the PT condition for this element (φ and driving force $\bar{X}$). In this way we have to check each FE of the admitted PT region.
(4) Sort FEs with respect to the criterion of the maximum driving force $\bar{X}$. The PT will occur in the element with the maximum driving forces $\bar{X}$. Prescribe the transformation strain ε_{02} for this element and repeat the solving of the elastoplastic problem. Calculate the stresses and strains of the new two-phase state of the sample. Thus, we define the FE where the PT occurs.
(5) Go back to step (2) and repeat the procedure to define the next FE where the PT will occur.

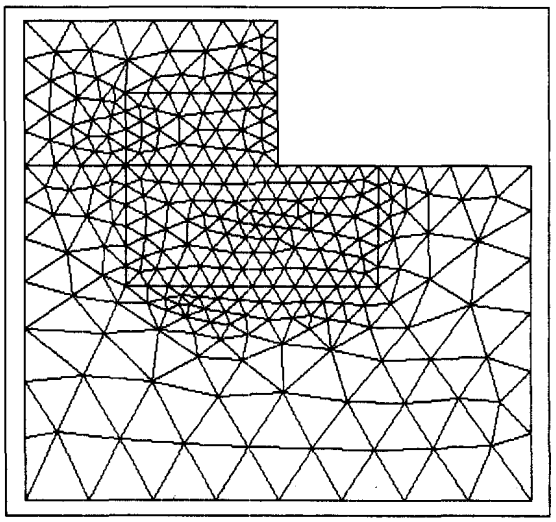

Fig. 22. Finite element mesh with refinement in the admitted PT region.

To decrease the calculation expenditure for searching for the next element, it is possible to decrease the number of FEs in the admitted PT region using calculated driving forces of a previous solution (e.g. only the elements with large value of driving forces for a previous solution and the elements surrounding the elements where the PT has already occurred are checked). We use the fact that PT in one element changes strain–stress state only in a limited region surrounding this element. Of course, when PT has occurred in a sufficiently large number of FEs, we should check the whole admitted PT region again. Thus, using this algorithm, we define the kinetics of growth of the PT zone. The solution algorithm for the problem is briefly presented in Fig. 23. Unfortunately, due to the complex structure of functional φ, it is not possible to simplify this procedure.

4.3.1. *The elastic matrix.* At first, the case of the elastic matrix is considered. Figure 24 shows us the progress of the PT region (with a sequentially increasing number of finite elements where PT occurs). The first nucleus appears at the edge of the sample (place of stress concentration) and all the sequential nuclei appear on the interface between the new and old phases. Thus, for this problem, in fact, the appearance and growth of one single connected region takes place. The values of work integral, φ, for every subsequent finite element where PT occurs, are presented as a diagram in Fig. 25; this diagram and PT condition $(11)_1$ demonstrate how the temperature of a sample should be varied for the progress of PT.

For instance, after the appearance of the first nucleus (at constant external conditions and $k = \text{const}$) the burst-like PT in the second and third elements occurs. The fourth element does not touch the corner point of the sample and the role of the stress concentrator decreases significantly. That is why φ decreases sharply and the external condition should be changed for the continuation of the PT.

The oscillated character of the diagram in Fig. 25 is often related to the case when two sides of a transforming triangle element are in contact with elements where PT has already occurred and for such an element the value of work integral, φ, is large (due to large negative initial stresses enforced by the transformation strain of surrounding transformed FEs). The analyses of PT progress is more complicated if k depends on a number of parameters (for example, on the volume of region where PT has occurred).

Let us analyze the reasons for the formation of a single connected region of a new phase. The stresses in transforming FE are a sum of initial stresses before PT (constant part) and finite increment during PT (changing part). If we have two phase material (matrix and nuclei) then, for negative transformation strain in nuclei, the pressure in the matrix has a minimum value near the interface and increases with an increase of the distance from the interface. Thus, initial negative pressure before PT in transforming FE (constant part)

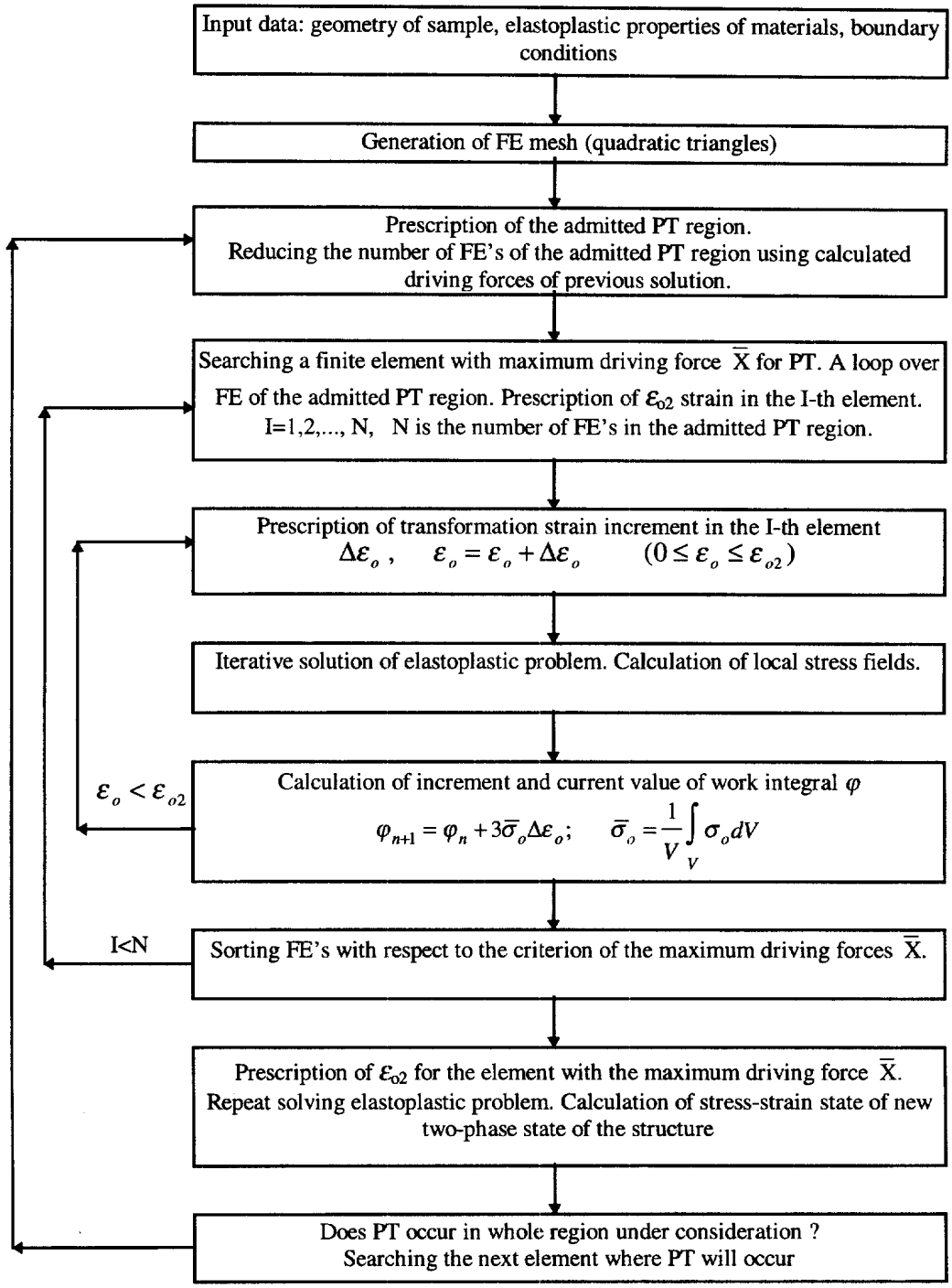

Fig. 23. Solution algorithm for phase transition in elastoplastic materials with progress of the PT region.

is the biggest for FEs near the interface between matrix and transformed FEs. The changing part of the pressure in FE during PT (for FEs within large elastic matrix) is approximately the same for different transforming FEs. Therefore, the work integral, φ, is bigger for the FE which is in contact with the transformed FEs and we obtain a single connected region for the elastic matrix.

4.3.2. *Elastoplastic matrix.* Figure 26 shows us the progress of the PT region for the elastoplastic matrix. In this case, the sequence of elements where PT occurs is more complicated than for an elastic matrix. At first, every new nucleus has the common boundary

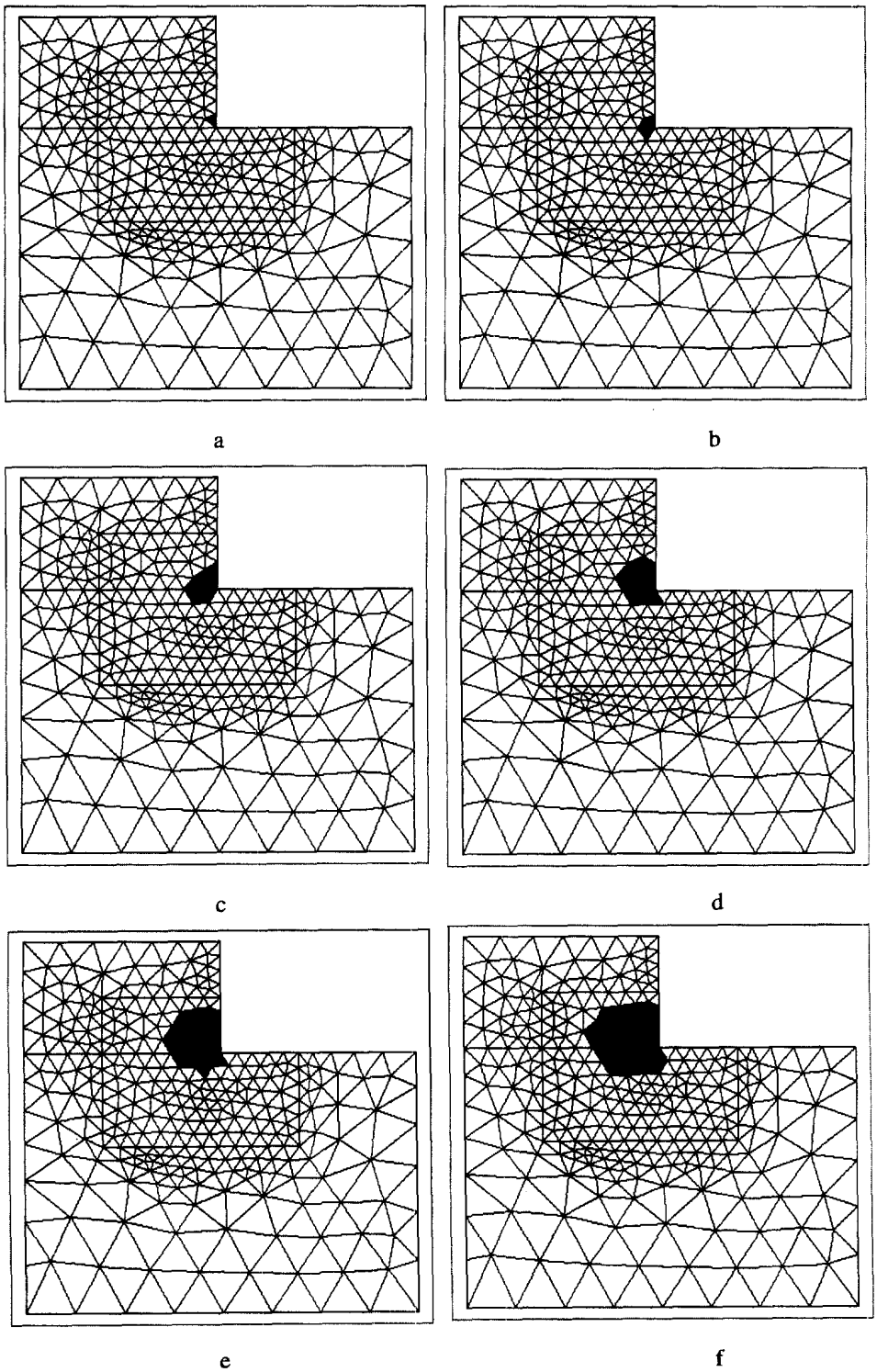

Fig. 24. Progress of phase transition in a sample at compression for an elastic problem. Transformed FEs are shaded.

with the old ones, but then the 12th element [Fig. 26(d)] forms another nucleus, which is not in contact with previous ones. With the progress of the PT region, new nuclei form a multiple-connected region. Such behavior of a sample is only forced by the distribution of local stresses in the elastoplastic matrix. As the new phase is elastic, then plastic stress relaxation occurs more easily when a new nucleus forms inside the matrix. As the internal stresses, due to a previously formed new phase, promote the formation of a single connected

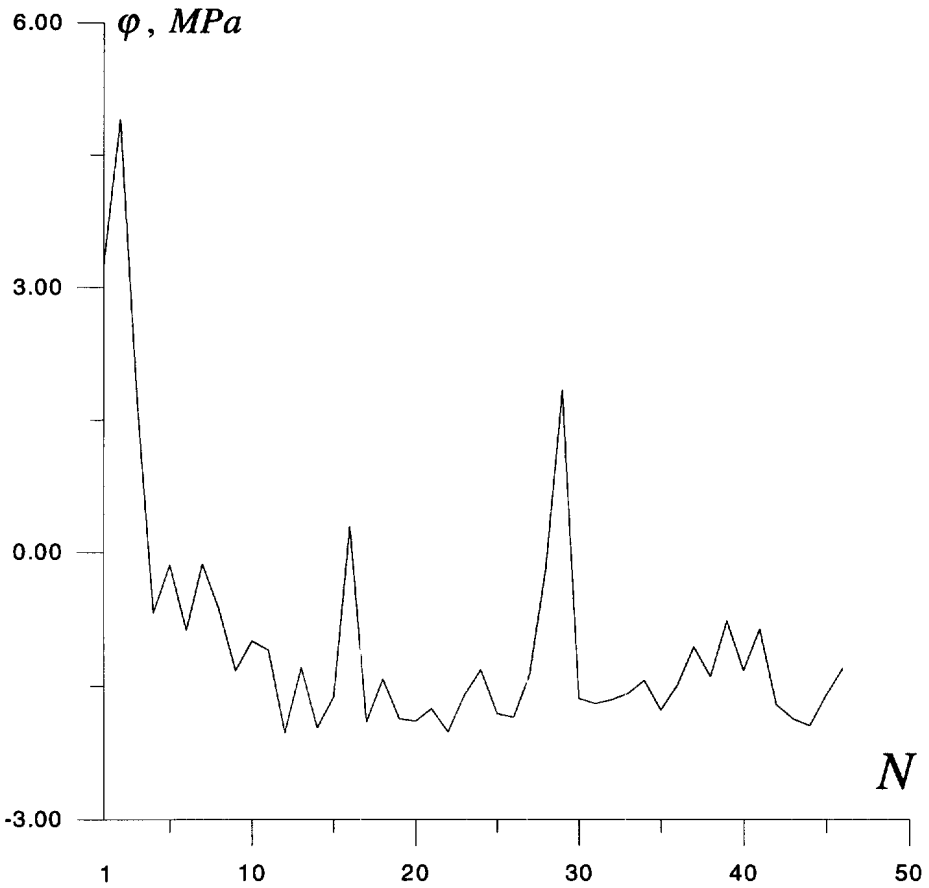

Fig. 25. Variation of the work integral φ in the course of PT for an elastic problem (N is the number of transforming FE).

region, then the combination of these two contributions determines whether the new region will be a single- or multiple-connected.

Now we analyze the reasons for the different shape of the transforming region for the cases of elastic and elastoplastic matrix. We can consider the above elastoplastic problem with $P = 0$ and $\sigma_y^m = 0$ (it is limit case), i.e. we have the problem of appearance of elastic nuclei in fluid (matrix) at zero pressure. Then the stresses in a single-connected region of the matrix will always be equal to zero during the PT, due to $\sigma_y^m = 0$. For any transforming FE which is not in contact with a transformed FE, the work integral, φ, is equal to zero (stresses in the transforming FE are zero, due to zero stresses at the interface matrix-transforming FE). For transforming FE, which is in contact with a transformed FE, the work integral φ, is negative (because of the jump of negative transformation strain across the interface between the two FEs and the condition of elasticity of these FEs according to the problem formulation internal stresses in transforming FE is nonzero). Thus, at $k = \text{const}$ and $\sigma_y^m = 0$ according to extremum principle (18) the shape of the new phase is more profitable when the nuclei do not touch one another. The effect of plasticity in this case (relaxation of stresses) is the same as the noncoherence effect. With varying yield stress of the matrix, σ_y^m, it is possible to change the value of the work integral, φ, for transforming the FEs and, consequently, the kinetics of the PT. Plasticity reduces both the constant part of pressure before PT (i.e. plasticity resists PT) and the changing part of pressure during PT (i.e. promotes PT).

The values of the work integral, φ, for every subsequent element where PT occurs are presented as a diagram in Fig. 27. The way of the analysis of the diagram is the same as for the case of the elastic matrix in Fig. 25.

It is necessary to note that the problems 4.3.1 and 4.3.2 are solved under the same external conditions and using the same finite element mesh. Preliminary investigations of

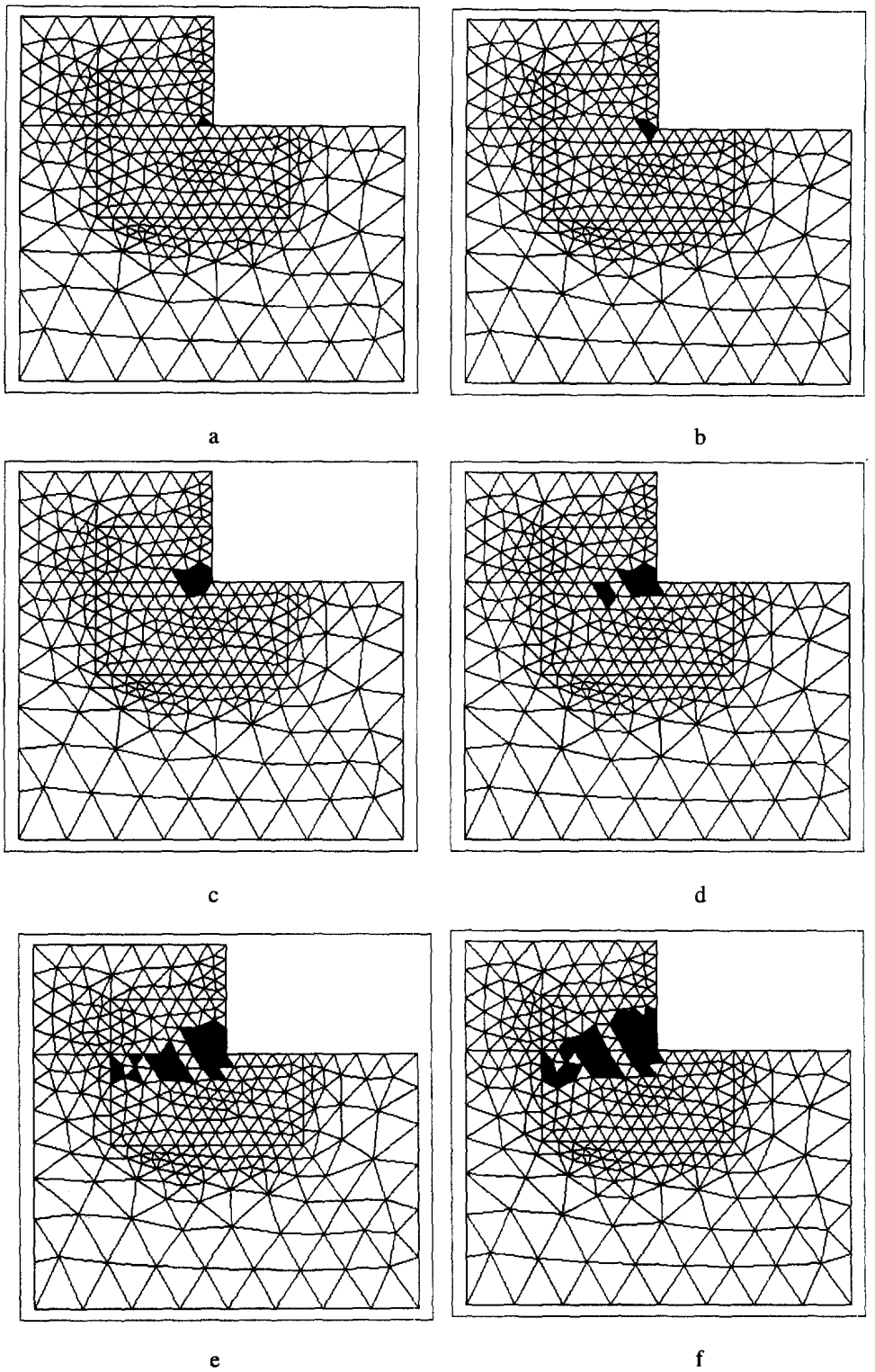

Fig. 26. Progress of phase transition in a sample at compression for an elastoplastic problem. Transformed FEs are shaded.

accuracy of numerical solutions showed that the maximum calculation error of the work integral, φ, is about 2–3% for elastic and 8–10% for elastoplastic materials. This error is related to the fact that at PT transformation strain is given only in one element. A decrease of the error can be achieved by increasing the polynomial order of FEs or dividing the

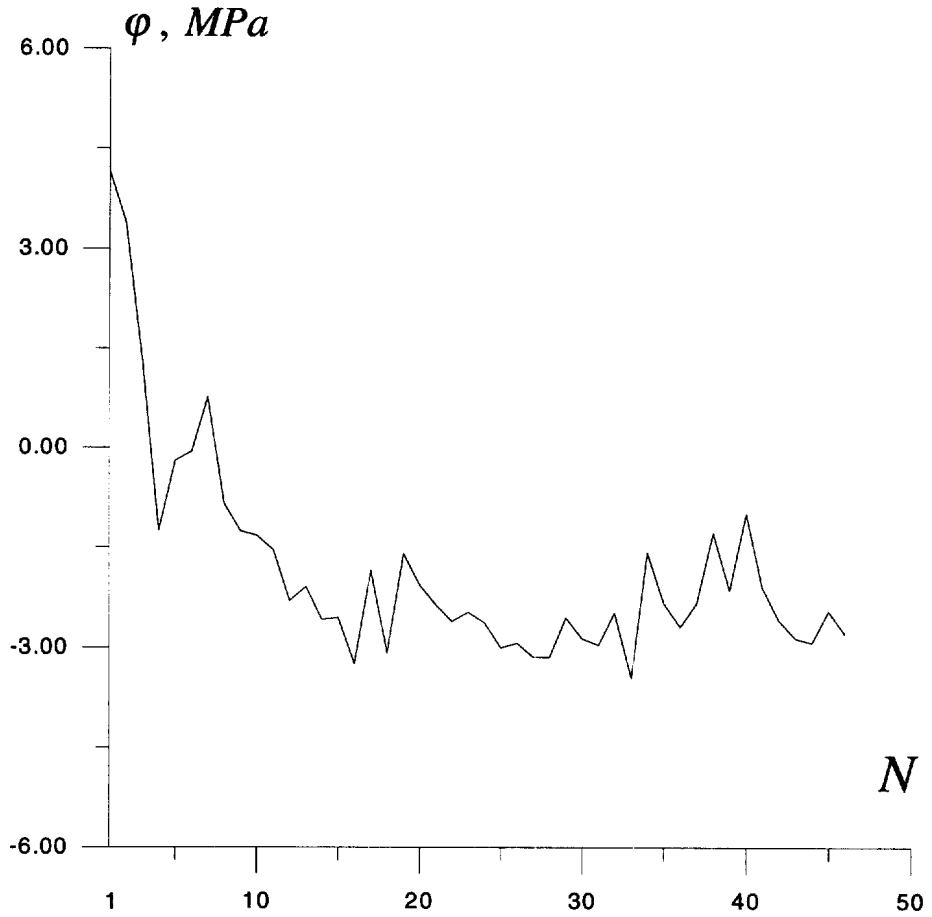

Fig. 27. Variation of the work integral φ in the course of PT for an elastoplastic problem (N is the number of transforming FE).

element into smaller ones, i.e. using auxiliary meshes. More elaborate analyses of solution error will be presented in a special paper.

5. CONCLUSIONS

(1) A numerical study of martensitic PT in elastoplastic materials, based on a new thermomechanical approach, is presented. PT condition based on the second law of thermodynamics and related maximum principle are used. Stress history (during transformation process) dependence is a characteristic feature of new PT criterion. A simple way for admitting noncoherence and fracture at the interface is proposed.

(2) Solution algorithms of model problems of PT in elastoplastic materials (coherent and noncoherent interface, interface with fracture, moving interface, progress of PT zone) with use of new PT criterion are suggested.

(3) Numerous problems, related to nucleation in cylindrical elastoplastic sample, are solved numerically by FEM. Conditions of nucleation in cylindrical elastoplastic sample were obtained at different values of compressive force and values of transformation strain (in cases of coherent and noncoherent interface as well as for interface with fracture). It is shown that noncoherent interface and fracture promote considerably nucleation. Progress of plastic strains (TRIP) in elastoplastic sample under cyclic appearance and disappearance of new phase nucleus at fixed external force is considered. It was found that increments of macroscopic plastic strain per cycle beginning from the second cycle are almost the same.

(4) The problem of the progress of PT (layer by layer), in a cylindrical sample with a moving coherent and noncoherent interface, is modeled. The driving force for the PT

grows during the coherent interface propagation, consequently at $k = \text{const}$ the PT should occur in the whole sample at fixed external parameters. It is shown that the noncoherent interface has low mobility or cannot move at all, which agrees with known experiments.

(5) The problem of the progress of the PT zone (element by element), in the sample with notch, is modeled. It is shown that for elastic materials the growth of a single-connected region of new phase occurs. For elastoplastic materials complex multiple-connected PT region (discrete microstructure) is obtained. It is related to the assumption that the new phase is elastic, consequently, plastic stress relaxation occurs more easily when a new nucleus has no contact with the previously formed new phase.

(6) It is planned to solve the problems of determination of microstructure of real material at PT (allowing for crystallography of transformation strain) using new thermomechanical criterion.

Let us compare our approach with the published ones [Ganghoffer *et al.* (1991); Marketz and Fischer (1994a, 1994b)], where the progress of PT (and, consequently, PT criterion) for coherent interfaces is estimated by the maximization of transformation work, $\boldsymbol{\sigma} : \boldsymbol{\varepsilon}_t$, where $\boldsymbol{\sigma}$ is the stress before PT. Of course, such an approach is much simpler, because for choosing the next transforming element it is not necessary to solve the large number of elastoplastic problems with trial transformation strain in each element. Stress conjugated with the transformation strain (in our case $\bar{\sigma}_0$) varies significantly with the growth of the transformation strain (especially for the coherent interface), changes the sign and the work integral, φ, has a completely different (much smaller) value than at constant $\bar{\sigma}_0$. Thus, in problem 4.1.1, at $P = 50$ MPa with fixed stress, we get $\varphi = 3 \cdot 50 \cdot 0.005 = 0.75$ MPa at $|\varepsilon_0| = 0.005$, but $\varphi = -0.3$ MPa in our case with changing stress states (Figs 6 and 7). Consequently, the results are qualitatively different. Since at constant $\boldsymbol{\sigma}$ the value φ is much bigger in the above-cited papers than in our case, PT can start earlier, at smaller $\bar{X}$ and probably at $\bar{X} < 0$, which is in contradiction with the second law of thermodynamics. Consequently, despite the fact that the numerical implementation of PT criterion $(11)_1$ is more complicated, other simpler ways can be qualitatively contradictory. Note, that we do not know other published results on PT in elastoplastic materials with crack or noncoherence at the interface.

Acknowledgement—We gratefully acknowledge the support of the Volkswagen Foundation, grant I/70283.

REFERENCES

Denis, S. (1996) Considering stress-phase transformation interactions in the calculation of heat treatment residual stresses. *Journal de Physique IV, Colloque C*1, supplément au *Journal de Physique III*, **6,** 159–174.

Ganghoffer, J. F., Denis, S., Gautier, E., Simon, A., Simonsson, K. and Sjöström, S. (1991) Micromechanical simulation of a martensitic transformation by finite element. *Journal de Physique IV, Colloque C*4, supplément au *Journal de Physique III*, **1,** 83.

Huo, Y. and Müller, I. (1993) Thermodynamics of pseudoelasticity—a graphical approach. *Continuum Mechanics and Thermodynamics*, **5,** 163–204.

Idesman, A. V. and Levitas, V. I. (1995) Finite element procedure for solving contact thermoplastic problems at large strain, normal and high pressures. *Computational Methods in Applied Mechanics and Engineering*, **126,** 39–66.

Inoue, T. and Raniecki, B. (1978) Determination of thermal hardening stress in steels by use of thermoplasticity theory. *Journal of Mechanical and Physical Solids*, **26,** 187–212.

Leblond, J. B., Devaux, J. and Devaux, J. C. (1989) Mathematical modeling of transformation plasticity in steels. Part I and II. *International Journal of Plasticity*, **5,** 551–591.

Levitas, V. I., Idesman, A. V., Leshchuk, A. A. and Polotnyak, S. B. (1989) Numerical modeling of thermomechanical processes in high pressure apparatus applied for superhard materials synthesis. *High Pressure Science and Technology, Proceedings of the X*1 *AIRAPT International Conference*, ed. N. V. Novikov, Vol. 4, pp. 38–40.

Levitas, V. I. (1992) *Thermomechanics of Phase Transformations and Inelastic Deformations in Microinhomogeneous Materials*. Naukova Dumka, Kiev.

Levitas, V. I. (1995a) Thermomechanics of martensitic phase transitions in elastoplastic materials. *Mechanical Research Communication*, **22,** 87–93.

Levitas, V. I. (1995b) Condition of nucleation and interface propagation in thermoplastic materials. *Journal de Physique IV, Colloque C*2, **5,** 41–46.

Levitas, V. I. (1995c) The postulate of realizability: formulation and applications to post-bifurcation behavior and phase transitions in elastoplastic materials. Part I and II. *International Journal of Engineering of Science*, **33,** 921–971.

Levitas, V. I., Stein, E. and Idesman, A. V. (1995) Phase transitions in elastoplastic materials: thermodynamical theory and numerical simulation. *Proceedings of IMMM'95*, pp. 581–586. Academic Publishers.

Levitas, V. I. (1996) Phase transitions in inelastic materials at finite strains: a local description. *Journal de Physique IV, Colloque C1*, supplément au *Journal de Physique III*, **6,** 55–64.

Levitas, V. I., Stein, E. and Lengnick, M. (1996) On a unified approach to the description of phase transitions and strain localization. *Archive Applied Mechanics*, **66,** 242–254.

Levitas, V. I. (1997a) Phase transitions in elastoplastic materials: continuum thermomechanical theory and examples of control. Part I and II. *Journal of Mechanical and Physical Solids* (in press).

Levitas, V. I. (1997b) Thermomechanical theory of martensitic phase transformations in inelastic materials. *International Journal of Solids and Structures* **35,** 889–940.

Marketz, F. and Fischer, F. D. (1994a) A micromechanical study on the coupling effect between microplastic deformation and martensitic transformation. *Computational and Material Science*, **3,** 307.

Marketz, F. and Fischer, F. D. (1994b) Micromechanical modelling of stress-assisted martensitic transformation. *Modelling Simulation Material Science Engineering*, **2,** 1017.

Mitter, W. (1987) *Umwandlungsplastizität und ihre Berücksichtigung bei der Berechnung von Eigenspannungen.* Stuttgart: Gebrüder Bornträger, Berlin.

Novikov, N. V., Levitas, V. I., Leshchuk, A. A. and Idesman, A. V. (1988) Simulation of diamond synthesis processes in a reaction zone of high pressure apparatus. *Doklady of the Ukrainian SSR Academy of Science*, Series A, **7,** 40–43.

Novikov, N. V., Levitas, V. I., Leshchuk, A. A. and Idesman, A. V. (1991) Mathematical modeling of diamond synthesis process. *High Pressure Research*, **7,** 195–197.

Padmanabhan, K. A. and Dabies, G. J. (1980) *Superplasticity*. Springer, Berlin.

Simonsson, K. (1994) Micromechanical FE-simulations of the plastic behavior of steels undergoing martensitic transformation. Dissertation no. 8. 362, Linköping.

Stringfellow, R. G., Parks, D. M. and Olson, G. B. (1992) A constitutive model for transformation plasticity accompanying strain-induced martensitic transformations in metastable austenitic steels. *Acta Metallica Materials*, **40,** 1703–1716.